

Analysis and Experimental Investiagtion of of Catalytic Converter with Ceramic Coating by Plasma Spray Coating

A PROJECT REPORT

Submitted by

G.SRINIVAS(211419114294)

J.SANTHOSH(211419114260)

A.SILAMBARASAN(211419114287)

STEPHIN ABRAHAM.S(211419114297)

in partial fulfillment for the award of the degree of

BACHELOR OF ENGINEERING

**IN
MECHANICAL ENGINEERING**



PANIMALAR ENGINEERING COLLEGE(An Autonomous
Institution, Affiliated to Anna University, Chennai)

APRIL& 2023

PANIMALAR ENGINEERING COLLEGE
(An Autonomous Institution, Affiliated to Anna University, Chennai)

BONAFIDE CERTIFICATE

Certified that this project report “Analysis and Experimental Investigation of Catalytic Converter with Ceramic Coating by Plasma Spray Coating”

is the bonafide work of “**G.SRINIVAS** (211419114294)

J.SANTHOSH (211419114260)

A.SILAMBARASAN (211419114287)

S.STEPHIN ABRAHAM (211419114297)

who carried out the project work under my supervision.

SIGNATURE

Dr. L. KARTHIKEYAN M.E, M.B.A, PhD Dr. A. PREMKUMAR, M.E., PhD

PROFESSOR & HEAD

Dept of Mechanical Engineering
Panimalar Engineering College
Bangalore trunk road
Varadharajapuram, Nasarethpettai
Poonamalle Chennai 23

SIGNATURE

Assistant Professor G1,

Dept. of Mechanical Engineering
Panimalar Engineering College
Bangalore trunk road
varadharajanpuram Nasarethpettai
Poonammalle Chennai 23

Submitted for Anna university project viva –voce held on 10.04.2023 during the Year 2022 – 2023.

INTERNAL EXAMINER

EXTERNAL EXAMINER

Abstract

Now a days the global warming and air pollution are big issue in the world. The 70% of air pollution is due to emissions from an internal combustion engine. The harmful gases like , NOX CO, unburned HC and particulate matter increases the global warming, so catalytic converter plays an vital role in reducing harmful gases, but the presence of catalytic converter increases the exhaust back pressure due to this the volumetric efficiency will decrease and fuel consumption is higher. So analysis of catalytic converter is very important. The rare earth metals now used as catalyst to reduce NOX are costly and rarely available. The scarcity and high demand of present catalyst materials necessitate the need for finding out the alternative materials or surface modification. therefore, the catalytic converter is modeled and analyzed with different ceramic powder's like alumina, Titania and zirconia by Ansys. With help of Ansys, may identify the best and suitable powder for catalytic converter, and this may coat with specimen substrate and subsequently testing may carried out like hardness, corrosion behavior and microstructural characterization with both coated and un coated substrate. The results may propose for optimized catalytic converter.

TABLE OF CONTENTS

CHAPTER NO	TITLE	PAGE NO
	LIST OF TABLES	
	LIST OF FIGURES	
I	INTRODUCTION	6
	1.1 introduction	
II	REVIEW OF LITERATURE	8
	2.1 Review of literature	
III	RESEARCH METHODOLOGIES	11
	3.1 Aim & Objectives	11
	3.2 Scope of the project	11
	3.3 Methodology	12
IV	WORKING PRINCIPLES	13
	4.1 Working principle	13
	4.2 Coating: an overview	13
	4.2.1 Coating technique	13
	4.2.2 Thermal spray technique	14
	4.2.3 Plasma coating process	15
	4.2.4 Pre-treatment process	16
	4.2.5 Characteristics of thermal spray coatings	18
V	COATING POWDER'S: AN OVERVIEW	21
	5.1 PROPERTIES OF ALUMINA	21
	5.2 ZIRCONIA	22
	5.2.1 Background	23
	5.2.2 Types of Zirconias	23

	5.2.3 Property Comparison	24
	5.2.4 Yttria (Y ₂ O ₃)	25
VI	SOFTWARE'S: AN OVERVIEW	
	6.1 CATIA	26
	6.2 ANSYS EVALUATION	28
	6.3 Element type used in the project	30
VII	EXPERIMENTAL WORK	
	7.1 BRINELL HARDNESS	44
	7.2 SALT SPRAY TEST	45
	7.2.1 Testing equipment	46
	7.2.2 Salt spray cabinet	47
	7.3 MICROSTRUCTURE	49
	7.3.1 Microscopy	50
	7.3.2 X-Ray microtomographic	50
	7.3.3 OPTICAL MICROSCOPY	51
VIII	CONCLUSION	58
	REFERENCE	59

CHAPTER - 1

INTRODUCTION

Internal Combustion engines generate undesirable emissions during the combustion process, which include, NOX CO, unburned HC, smoke etc. Apart from these unwanted gases, it produces Particulate Matter (PM) such as lead, soot. All these pollutants are harmful to environment and human health. They are the main causes for greenhouse effect, acid rain, global warming etc. The simplest and the most effective way to reduce NOX and PM, is to go for the after treatment of exhaust. Devices developed for after treatment of exhaust emissions includes thermal converters or reactors, traps or filters for particulate matters and catalytic converters. The most effective after treatment for reducing engine emission is the catalytic converter found on most automobiles and other modern engines of medium or large size. The catalyst and filter materials placed inside the catalytic converter increase back pressure. This increase in back pressure causes more fuel consumption, and in most cases, engine stalling might happen. The filtration efficiency and back pressure are interrelated. If maximum filtration efficiency using very fine grid size wire meshes, is achieved, the back pressure will also be increased, which causes more fuel consumption. On the other hand, if larger grid size wire meshes are used, back pressure will be less, but the filtration efficiency will also be reduced, which does not help in meeting the present emission norms. With the help of CFD analysis, it is attempted to find out the optimum solution to get maximum filtration efficiency with limited back pressure developed inside the catalytic converter.

Selection of filter material

There are many types of filter materials are used in internal combustion engine. They are Ceramic monolith, ceramic foam, steel wire meshes, ceramic silicon fiber, porous ceramic honey comb are the few types of filter materials. Out of these filter materials, steel wire mesh is selected as filter material because knitted steel wire mesh material is ranked first for its collection efficiency of particulate matter.

The other reasons for its selection are, · Thermal stability during regeneration. · Good mechanical properties. · Long durability. · Easy availability and less cost

Diesel power inevitably finds a very important role in the development of the plant's economy and technical growth. In spite of their high thermal efficiency, one cannot ignore the fact about the effect of their exhaust, in the atmosphere. It is a well-known fact that the toxic gases emitted in diesel engines are less than the engines. Due to high cost of petrol, diesel engines are more in use. Anticipating the use of diesel engines, even more in the near future; this system developed can be used to control the toxic gases, coming out of the diesel engines.

These toxic gases are harmful not only to the atmosphere, but also to the human & animal race. Objective of this project is to design & fabricate a simple system, where the toxic levels are controlled through chemical reaction to more agreeable level. This system acts itself as a silencer; there is no need to separate the silencer. The whole assembly is fitted in the exhaust pipe; it does not give rise to any complications in assembling it. This system is VERY COST EFFECTIVE AND MORE ECONOMICAL.

Diesel engines are playing a vital role in Road and sea transport, Agriculture, mining and many other industries. Considering the available fuel resources and the present technological development, Diesel fuel is evidently indispensable. In general, the consumption of fuel is an index for finding out the economic strength of any country. In spite, we cannot ignore the harmful effects of the large mass of the burnt gases, which erodes the purity of our environment everyday.

It is especially so, in most developed countries like USA and EUROPE. While, constant research is going on to reduce the toxic content of diesel exhaust, the diesel power packs find the ever increasing applications and demand. This project is an attempt to reduce the toxic content of diesel exhaust, before it is emitted to the atmosphere. This system can be safely used for diesel power packs which could be used in inflammable atmospheres, such as refineries, chemicals processing industries, open cast mines and other confined areas, which demands the need for diesel power packs.

CHAPTER - 2

LITERATURE REVIEW

S. Sendilvelan et. al., (2017) The objective of this paper is to calculate various emission factors in diesel engine using cerium oxide nanoparticles. Cerium oxide used in the form of nanoparticles. Experimental results revealed that emission level decreased upto 98% when cerium oxide used to convert oxides of Nitrogen, Hydrocarbon and Carbon Monoxide levels at 440 degree temperature. The cerium oxide increase the conversion rate due to the oxygen content for the oxidation process of carbon monoxide and hydrocarbon in the catalytic converter. It was also observed that the cerium nanoparticles reduce the oxides of nitrogen effectively.

Rahul Ganji et. al., (2017) This paper discusses about the implementation of three way converter. Here, bio catalytic converter is used. Algae was used as fuel as algae has great potential in reducing gaseous emissions. This catalytic converter has three algae chambers connected to it. In this, emission reduction pipe is used to expand gases before entering into bio catalytic converter. It is observed that there is a reduction of 70% HC and 36.3% CO against the regulation standards with bio catalytic converter.

R. Praveen et. al., (2014) This paper discusses about using urea solution as a reduction catalyst to reduce NO_x emissions. An aqueous solution of urea was injected in engine exhaust pipe for reducing NO_x emissions in single cylinder light duty stationery DI diesel engine fuelled with diesel and diesel- (10%) ethanol blend. A concentration of urea solution varying from 30 to 35% by weight with constant flow rates and tested with fitting Titanium dioxide (TiO₂) coated catalyst which controls by products of ammonia and water vapour. Results indicated that a maximum of 70 % of NO_x reduction was achieved an engine fuelled with diesel-ethanol blend and constant flow rate of 0.75 lit/hr with an urea concentration of 35% and 66% NO_x.

S. P. Venkatesan et. al., (2017) The main aim of this paper is to fabricate system, where the level of intensity of toxic gases is controlled through chemical reaction to more agreeable level. This system acts itself as an exhaust system; hence there is no needs to fit separate the silencer. The whole assembly is fitted in the exhaust pipe from engine. In this paper, catalytic converter with copper oxide as a catalyst, by replacing noble catalysts such as platinum, palladium and

rhodium is fabricated and fitted in the engine exhaust. With and without catalytic converter, the experimentations are carried out at different loads such as 0%, 25%, 50%, 75%, and 100% of maximum rated load.

B. Bala Krishna et. al., (2014) The catalyst and filter materials placed inside the catalytic converter increase back pressure. In this paper, knitted steel wire mesh used as the filter material. Analysis of this model is done in CFD. Attempt is made to analyze the Catalytic Converter and to find optimum solution to get maximum filtration efficiency with limited back pressure. It is concluded that the catalytic converter 90mm-MC-2 has the lowest pressure drop among the catalytic converter with different wire mesh grid sizes, due to lower pressure drop the fuel consumption become lower and volumetric efficiency becomes higher.

P. Karuppuswamy et. al., (2013) This paper deals with the design and analysis of Catalytic Converter. As this component increases back pressure, this paper analysed various models and studied mainly two parameters, filtration efficiency and back pressure. Softwares used are CFD, Star CMM+. The back pressure variations in various models and the flow of the gas in the substrate were discussed in. Finally, the model with limited backpressure was fabricated and Experiments were carried out on computerized r single cylinder four stroke diesel engine test rig with an eddy current dynamometer. The performance of the engine and the catalytic converter were discussed.

S. Sendilvelan, K. Bhaskar and S. Nallusamy, Experimental investigation on cerium oxide nanoparticles with alumina catalytic converter to increase emission conversion efficiency in automobiles, Rasayan Journal of Chemistry, June 2017

Rahul Ganji, VN Yenugula, Emission reduction in automobile engine exhaust using bio catalytic converter: An Experimental Study, IOSR Journal of Mechanical and Civil Engineering (IOSR-JMCE), Dec 2017

R. Praveen, S. S. Natarajan, *Experimental study of Selective Catalytic Reduction system on CI Engine fuelled with Diesel – Ethanol blend for NO_x reduction with injection of urea solutions, International Journal of Engineering and Technology (IJET), May 2014*

S. P. Venkatesan, B. Venusai, G. Sanjeeth, K. Saikarthik and A. Sivakrishna Reddy, *emissions study on copper oxide catalytic converter Fitted diesel engine, ARPN Journal of Engineering and Applied Sciences, June 2017*

B.Balakrishna and Srinivasarao Mamidala, *Design Optimization of Catalytic Converter to reduce Particulate Matter and Achieve Limited Back Pressure in Diesel Engine by CFD, International Journal of Current Engineering and Technology, February 2014*

P.Karuppusamy, Dr. R.Senthil, *Design and analysis of flowcharacteristics of catalytic converter and effects of backpressure on engine performance, International Journal of Research in Engineering & Advanced Technology (IJREAT) March, 2013*

CHAPTER - 3

3.1 AIM & OBJECTIVES

To study the functional characteristics of the catalytic converter

To design the catalytic converter with solidworks software

To investigate the thermal analysis of catalytic converter with different ceramic powder such as Alumina , Titania and Zirconia.

Coat the sample with best identified powder

Conduct the hardness, corrosion and microstructural characterization of coating and uncoated powder.

To compare the results with uncoated catalytic converter

To identify the suitable ceramic powder for catalytic converter.

3.2 SCOPE OF THE PROJECT

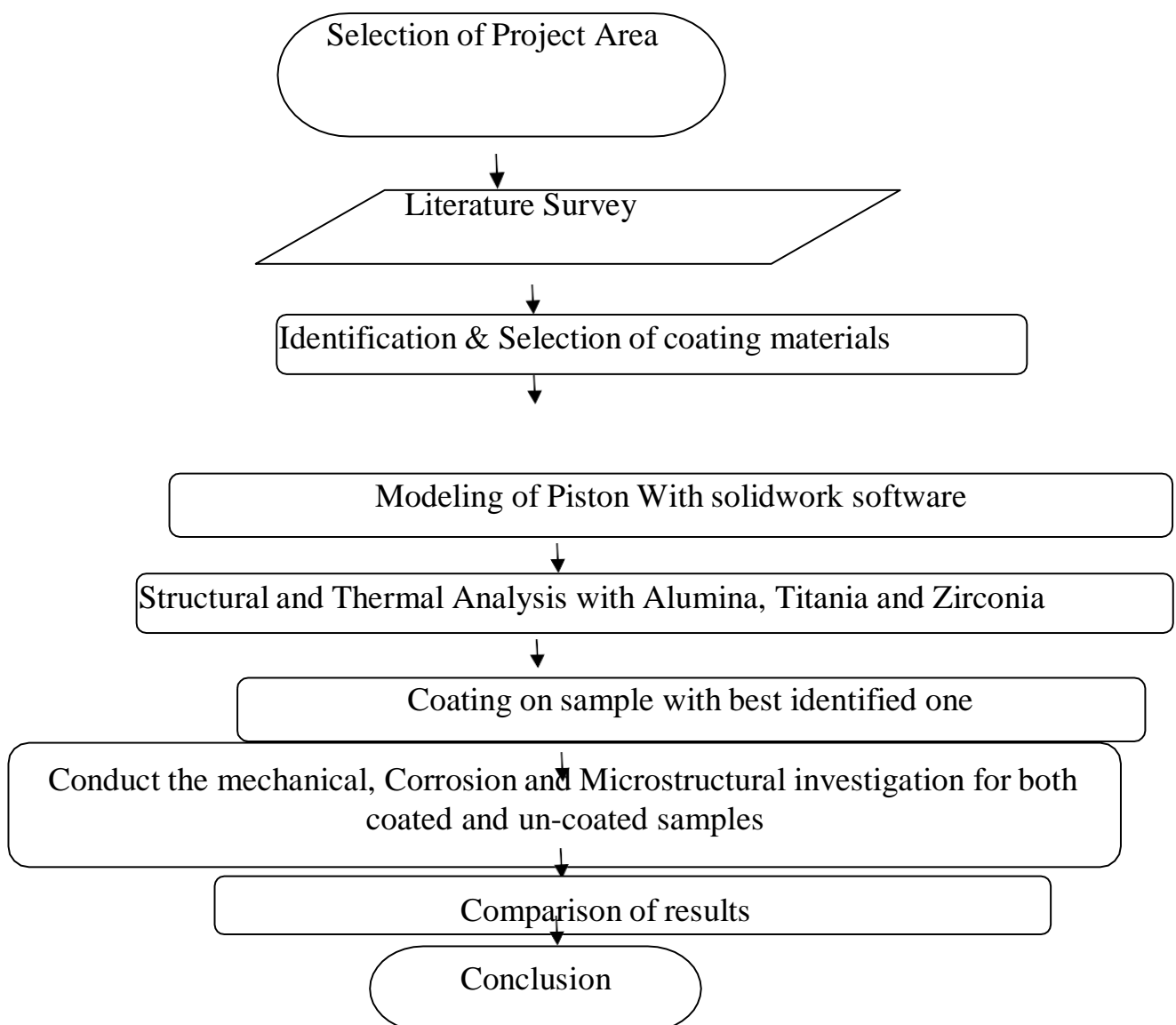
Coating is a covering that is applied to an object. The aim of applying coatings is to improve surface properties of a bulk material usually referred to as a substrate. One can improve the hardness, appearance, adhesion, wet ability, corrosion resistance, wear resistance, scratch resistance, etc,

3.3 METHODOLOGY

METHODOLOGY

Modeling and analysis of 3-D models of the Piston were carried out using ANSYS FEA.

The methodology includes the process of numerical analysis and experimental investigation and comparison with different ceramic coated piston by Ansys and experimental investigations.



CHAPTER - 4

4.1 WORKING PRINCIPLE:

The high temperature high pollutant exhaust gas is allowed to pass through the belt – mouth assembly of the scrubber in the first phase. The bell – mouth at the inlet/outlet is approximately 2 ½ times more in an area is that of the inlet. This allows the exhaust gas to expand considerably. This expansion allows the gas to cool, because the temperature is a function of pressure. This considerable reduction of backpressure allows for the additional involved due to the introduction of water and lime stone container. The venture effect of the bell – mouth is minimized because the exhaust gas escapes out of the bell – mouth randomly along the periphery.

After expansion, the emission comes in contact with oil; (which could be otherwise being any alkaline solution) where the obnoxious products of combustion are scrubbed when bubbled through it. The bell – mouth also allows for more contact area with water, so that effective cooling takes place with in the short span of time available for the gas to pass through the oil. The length of bubbling can be increased by the oil level in the scrubber tank. But this will be increased result in an abnormal backpressure, which inadvertently affect the performance of the engine. And for this reason the bell – mouth is a multipurpose component, to allow for reduction in back pressure, and provides for an increased contact area with the scrubbing agent.

After bubbling through the oil, it comes in contact with bubbles, which encourage turbulence of the exhaust gas with in and below the oil surface without unduly increasing the back pressure of the exhaust. This allows for the thorough scrubbing of the emission, so that more obnoxious product is absorbed in the allowed time. The baffles are of invaluable help to reduce the carry over of oil particles which are converted into steam, which otherwise will escape out of the system. The filter is used to filter the carbon particles in the exhaust gas.

4.2 COATING: AN OVERVIEW

4.2.1 COATING TECHNIQUE

Coating is a covering that is applied to an object. The aim of applying coatings is to improve surface properties of a bulk material usually referred to as a substrate. One can improve appearance, adhesion, wetability, corrosion resistance, wear resistance, scratch resistance, etc.. They may be applied as liquids, gases or solids. Coatings can be measured

and tested for proper opacity and film thickness by using a Drawdown card.

4.2.3 THERMAL SPRAY TECHNIQUE

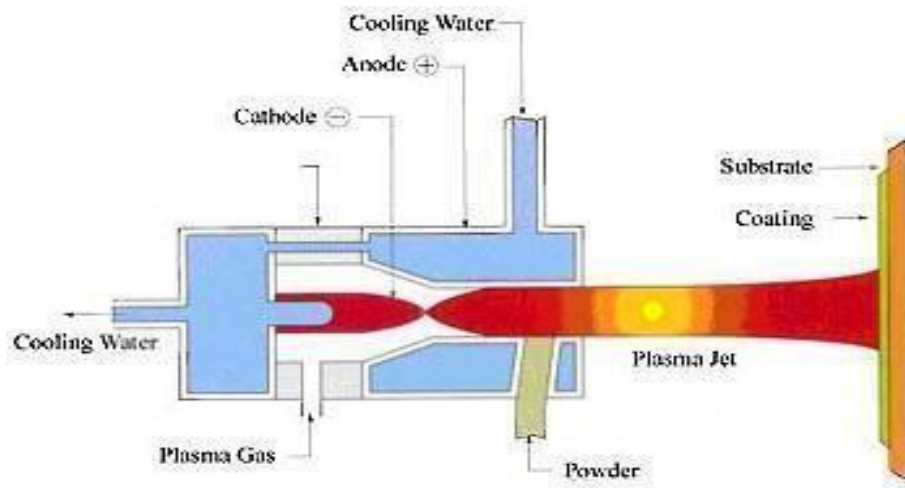


Fig.4.1 Thermal Spray Technique

Thermal spray is a surface treatment process that the subtle and dispersed metal or non-metallic coating material like wire or powder in a melt or semi-molten state, deposits on the substrate surface to form a sort of deposited layer.

Thermal spray material is heated to a plastic or molten state and then accelerated. While these particles hitting the substrate surface, they are deformed due to pressure, form layered sheet, and adhere to the substrate surface. They continuously accumulate and eventually form a layered coating. By changing coating materials, different functions can be realized such as erosion resistance, abrasion resistance, heat insulation, ceramic insulation and so on. Today, as a high-tech technique, thermal spray has been widely used in aerospace, automotive, energy, metallurgy, paper making, machinery maintenance, municipal construction and other areas.

In engineering and mechanical surface treatment areas, thermal spray technology is the most effective, economic and direct process to enhance the surface functions and parameters. Through the use of thermal spray technique, it can improve the life of equipment or spare parts, improve the surface performance, as well as reduce production

and maintenance costs. Thermal spray features include: abrasion resistance, heat-resistant barrier; anti-erosion; restore size; gap control; change in electrical conductivity, etc.

4.2.2 PLASMA COATING PROCESS

In all thermal spray techniques, plasma spray is the most flexible one as it can reach a sufficient temperature to melt or heat any material, so the coating material types are almost unlimited. Plasma spray gun is composed of a small chamber with a cathode (electrode) and an anode (nozzle).

Broken down by high-intensity arc, the gas through the chamber forms plasma substance, and releases large amount of heat, which can reach the temperature of $6000\text{ }^{\circ}\text{C}$ ~ $16000\text{ }^{\circ}\text{C}$. When the coating material is high-speedily injected into the gas flame, it is melted and impacts on the substrate surface.

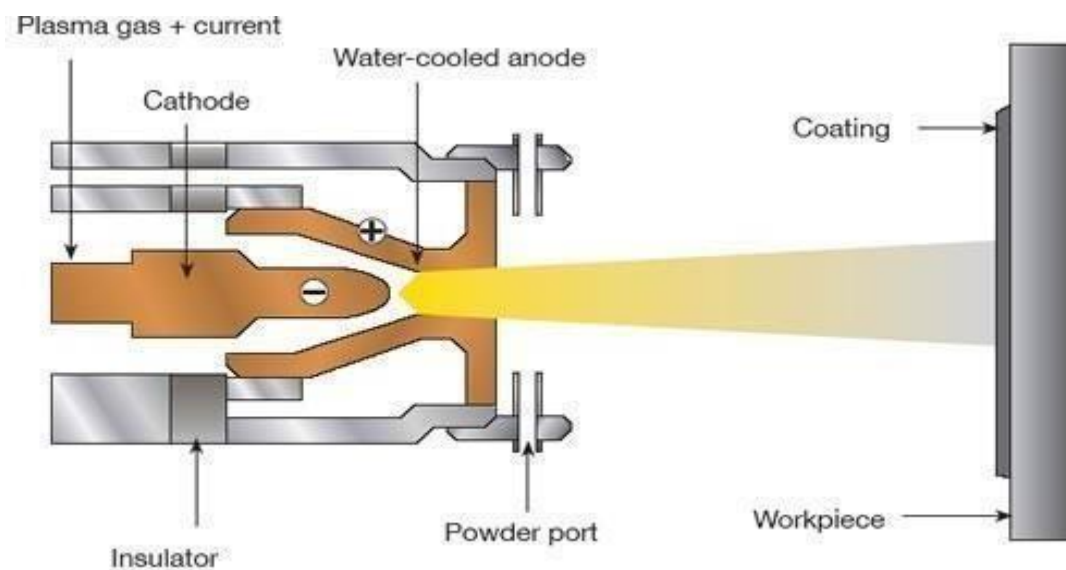


Fig.4.2 Plasma Spraying

We offer Plasma Spraying service using SulzerMetco equipment comprising of a number of SulzerMetco units including a 3MB unit feeding a MBN gun and a 7MB unit feeding a 9MB gun is used in this project for the purpose of coating. A wide range of coatings can be applied including ceramics, zirconium, yttrium, chrome carbides &

tungsten carbide and used in a wide range of applications including seal diameters, machines spindles & print rollers.

4.3.2 OVERVIEW OF PLASMA COATING PROCESS

The plasma coating process is basically a high frequency arc, which is ignited between an anode and a tungsten cathode. The gas flowing through between the electrodes (i.e., He, H₂, N₂ or mixtures) is ionized such that a plasma plume several centimeters in length develops. The temperature within the plume can reach as high as 16,000° K.

The sprayed material (in powder form) is injected into the plasma plume where it is melted and propelled at high speed to the substrate surface where it rapidly cools and forms the coating. Heat from the hot particles is transferred to the cooler base material. As the particles shrink and solidify, they bond to the roughened base material. Adhesion of the coating is therefore based on mechanical “hooking”. The plasma spraying process is classed as a cold process and because of this damage and distortion etc. can be avoided to the huge range of substrates we can coat.

4.2.4 PRE-TREATMENT PROCESS

Surface adhesion is purely mechanical and as such, a solid key is required, free of grease or other contaminants. Therefore the careful cleaning and pre-treatment of the surface to be coated is extremely important. Surface roughening usually takes place via grit blasting with dry corundum. In addition, other media, such as chilled iron, steel grit or SiC are used for some applications.

All items are grit blasted with sharp abrasive grit to achieve a surface roughness of approximately 100-300µin. Besides the type of grit, other important factors include particle size, particle shape, blast angle, pressure and purity of the grit media. Suitable substrate materials are those that can withstand blasting procedures to roughen the surface, generally having a surface hardness of about 55 Rockwell C or lower. Special processing techniques are required to prepare substrates with a higher hardness. General Parameters In The Process

Roughness of the substrate surface A rough surface provides a good coating adhesion. Cleanliness of the substrates The substrate to be sprayed on must be free from any dirt or grease or any other material that might prevent intimate contact of the splat and the substrate.

Cooling water: For cooling purpose distilled water should be used, whenever possible. normally a small volume of distilled water is re-circulated into the gun and it is cooled by an external water supply from a large tank. Sometime water from a large external tank is pumped directly into the gun.

Process parameters: In plasma spraying one has to deal with a lot of process parameters, which determine the degree of particle melting, adhesion strength and deposition efficiency of the powder. Deposition efficiency is the ratio of amount of powder deposited to the amount fed to the gun.

Arc power: It is the electrical power drawn by the arc. The power is injected in to the plasma gas, which in turn heats the plasma stream.

Plasma gas: Normally nitrogen or argon doped with about 10% hydrogen or helium is used as a plasma gas. The major constituent of the gas mixture is known as primary gas and the minor is known as the secondary gas.

Carrier gas: Normally the primary gas itself is used as a carrier gas. The flow rate of the carrier gas is an important factor. A very low flow rate cannot convey the powder effectively to the plasma jet, and if the flow rate is very high then the powders might escape the hottest region of the jet.

Mass flow rate of powder: Ideal mass flow rate for each powder has to be determined. a very high mass flow rate may give rise to an incomplete melting resulting in a high amount of porosity in the coating
Spraying angle: This parameter is varied to accommodate the shape of the substrate the coating porosity is found to increase as the spraying angle is increased from 30° to 60°. Beyond 60° the porosity level remains unaffected by a further increase in spraying angle. The spraying angle also affects the adhesive strength of the coating.

Thermal Spray is a generic term for a group of coating processes used to apply metallic or nonmetallic coatings. These processes are grouped into three major categories: flame spray, electric arc spray, and plasma arc spray. These energy sources are used to heat the coating material (in powder, wire, or rod form) to a molten or semimolten state. The resultant heated particles are accelerated and propelled toward a prepared surface by either process gases or atomization jets. Upon impact, a bond forms with the surface, with subsequent particles causing thickness buildup and forming a lamellar structure.

The thin “splats” undergo very high cooling rates, typically in excess of 10⁶ K/s for metals .

A major advantage of thermal spray processes is the extremely wide variety of materials that can be used to produce coatings . Virtually any material that melts without decomposing can be used. A second major advantage is the ability of most thermal spray processes to apply coatings to substrates without significant heat input. Thus, materials with very high melting points, such as tungsten, can be applied to finely machined, fully heat-treated parts without changing the properties of the part and without excessive thermal distortion of the part.

A third advantage is the ability, in most cases, to strip off and recoat worn or damaged coatings without changing part properties or dimensions. A disadvantage is the line-of-sight nature of these deposition processes. They can only coat what the torch or gun can “see.” Of course, there are also size limitations. It is impossible to coat small, deep cavities into which a torch or gun will not fit. The article “Introduction to Processing and Design” in this Handbook provides a more complete discussion of the advantages and disadvantages of thermal spray processes.

4.2.5 CHARACTERISTICS OF THERMAL SPRAY COATINGS

Microstructural Characteristics. The term “thermal spray” describes a family of processes that use the thermal energy generated by chemical (combustion) or electrical (plasma or arc) methods to melt, or soften, and accelerate fine dispersions of particles or droplets to speeds in the range of 50 to >1000 m/s (165 to >3300 ft/s).

The high particle temperatures and speeds achieved result in significant droplet deformation on impact at a surface, producing thin layers or lamellae, often called “splats,” that conform and adhere to the substrate surface.

Solidified droplets build up rapidly, particle by particle, as a continuous stream of droplets impact to form continuous rapidly solidified layers. Individual splats are generally thin (~ 1 to $20\text{ }\mu\text{m}$), and each droplet cools at very high rates ($>10^6\text{K/s}$ for metals) to form uniform, very fine-grained, polycrystalline coatings or deposits. Figure 2 shows a schematic of a generic thermal spray powder consolidation process, illustrating the key features and a typical deposit microstructure.

Sprayed deposits usually contain some level of porosity, typically between 0 and $\sim 10\%$, some unmelted or partially melted particles, fully melted and deformed “splats,” metastable phases, and oxidation from entrained air. Thermal spray process jets or plumes are characterized by large gradients of both temperature and velocity. Feedstock is usually in powdered form with a distribution of particle sizes. When these powdered materials are fed into the plume, portions of the powder distribution take preferred paths according to their inertia.

As a result, some particles may be completely unmelted and can create porosity or become trapped as “unmelts” in the coating. Use of wire and rod feedstock materials produces particle size distributions because of nonuniform heating and unpredictable drag forces, which shear molten material from the parent wire or rod.

The level of these coating defects varies depending on the particular thermal spray process used, the operating conditions selected, and the material being sprayed, as described later. Thermal spray coatings may contain varying levels of porosity, depending on the spray process, particle speed and size distribution, and spray distance.

Porosity may be beneficial in tribological applications through retention of lubricating oil films. Porosity also is beneficial in coatings on biomedical implants. Lamellar oxide layers can also lead to lower wear and friction due to the lubricity of some oxides. The porosity of thermal spray coatings is typically $<5\%$ by volume. The retention of some unmelted and/or resolidified particles can lead to lower deposit cohesive strengths, especially in the case of “as-sprayed” materials with no postdeposition heat treatment or fusion. Other key features of thermal spray deposits are their generally very fine grain structures and columnar orientation (Fig. 1b).

Thermal-sprayed metals, for example, have reported grain sizes of $<1\text{ }\mu\text{m}$ prior to postdeposition heat treatment. Grain structure across an individual splat normally ranges from 10 to $50\text{ }\mu\text{m}$, with typical grain diameters of 0.25 to $0.5\text{ }\mu\text{m}$, owing to the high cooling

rates achieved (~10⁶ K/s). The tensile strengths of as-sprayed deposits can range from 10 to 60% of those of cast or wrought materials, depending on the spray process used. Spray conditions leading to higher oxide levels and lower deposit densities result in the lowest strengths. Controlled-atmosphere spraying leads to ~60% strength, but requires postdeposition heat treatment to achieve near 100% values.

Low as-sprayed strengths are related somewhat to limited intersplat diffusion and limited grain recrystallization during the rapid solidification characteristic of thermal spray processes. The primary factor limiting adhesion and cohesion is residual stress resulting from rapid solidification of the splats.

Accumulated residual stress also limits thickness build-up Thermal Spray Processes and Techniques Members of the thermal spray family of processes are typically grouped into three major categories: flame spray, electric arc spray, and plasma arc spray, with a number of subsets falling under each category. (Cold spray is a recent addition to the family of thermal spray processes. This process typically uses some modest preheating, but is largely a kinetic energy process. The unique characteristics of cold spray are discussed in the article “Cold Spray Process” in this Handbook.) A brief review of some of the more commercially important thermal spray processes is given below.

CHAPTER - 5

COATING POWDER'S : AN OVERVIEW

5.1 PROPERTIES OF ALUMINA

Aluminium oxide is a chemical compound of aluminium and oxygen with the chemical formula Al_2O_3 . It is the most commonly occurring of several aluminium oxides, and specifically identified as aluminium(III) oxide. It is commonly called alumina, and may also be called aloxide, aloxite, or alundum depending on particular forms or applications. It commonly occurs in its crystalline polymorphic phase $\alpha\text{-Al}_2\text{O}_3$, in which it comprises the mineral corundum, varieties of which form the precious gemstones ruby and sapphire. Al_2O_3 is significant in its use to produce aluminium metal, as an abrasive owing to its hardness, and as a refractory material owing to its high melting point.

Al_2O_3 is an electrical insulator but has a relatively high thermal conductivity ($30 \text{ W m}^{-1} \text{ K}^{-1}$ [3]) for a ceramic material. Aluminum oxide is insoluble in water. In its most commonly occurring crystalline form, called corundum or α -aluminium oxide, its hardness makes it suitable for use as an abrasive and as a component in cutting tools.

Aluminium oxide is responsible for the resistance of metallic aluminium to weathering. Metallic aluminium is very reactive with atmospheric oxygen, and a thin passivation layer of aluminium oxide (4 nm thickness) forms on any exposed aluminium surface. http://en.wikipedia.org/wiki/Aluminium_oxide This layer protects the metal from further oxidation. The thickness and properties of this oxide layer can be enhanced using a process called anodising. A number of alloys, such as aluminium bronzes, exploit this property by including a proportion of aluminium in the alloy to enhance corrosion resistance. The aluminium oxide generated by anodising is typically amorphous, but discharge assisted oxidation processes such as plasma electrolytic oxidation result in a significant proportion of crystalline aluminium oxide in the coating, enhancing its hardness.

PROPERTIES OF TITANIA

Titanium dioxide, also known as titanium(IV) oxide or titania, is the naturally occurring oxide of titanium, chemical formula TiO_2 . When used as a pigment, it is called titanium white, Pigment White 6 (PW6), or CI 77891. Generally it is sourced from ilmenite, rutile and anatase. It has a wide range of applications, from paint to sunscreen to food colouring.

Titanium dioxide occurs in nature as well-known minerals rutile, anatase and brookite, and additionally as two high pressure forms, a monoclinic baddeleyite-like form and an orthorhombic α -PbO₂-like form, both found recently at the Ries crater in Bavaria. It is mainly sourced from ilmenite ore. This is the most widespread form of titanium dioxide-bearing ore around the world. Rutile is the next most abundant and contains around 98% titanium dioxide in the ore. The metastable anatase and brookite phases convert irreversibly to the equilibrium rutile phase upon heating above temperatures in the range 600°-800 °C.

Titanium dioxide has eight modifications – in addition to rutile, anatase, and brookite, three metastable phases can be produced synthetically (monoclinic, tetragonal and orthorhombic), and five high-pressure forms (α -PbO₂-like, baddeleyite-like, cotunnite-like, orthorhombic OI, and cubic phases) also exist:

Titanium dioxide

Chemical Compound

1. Titanium dioxide, also known as titanium oxide or titania, is the naturally occurring oxide of titanium, chemical formula TiO₂. When used as a pigment, it is called titanium white, Pigment White 6, or CI 77891. Wikipedia
- 2.
3. Formula: TiO₂
4. Molar mass: 79.866 g/mol
5. Melting point: 1,843 °C
6. Density: 4.23 g/cm³
7. Boiling point: 2,972 °C
8. IUPAC ID: Titanium dioxide, Titanium(IV) oxide

5.2 ZIRCONIA

Zirconia can be found in three crystal structures. These are monoclinic (m), tetragonal (t) and cubic (c) structures. Monoclinic structure is stable between room temperature and 1170 °C while it turns to tetragonal structure above 1170 °C. Tetragonal structure is stable up to 2379 °C and above this temperature, the structure turns to cubic structure. Zirconia (ZrO₂) is a ceramic material with adequate mechanical properties for manufacturing of medical devices. Zirconia stabilized with Y₂O₃ has the best properties for these applications. When a stress occurs on a ZrO₂ surface, a crystalline modification opposes the propagation of cracks. Compression resistance of ZrO₂ is about 2000 MPa. Zirconia is a crystalline dioxide of

zirconium. Its mechanical properties are very similar to those of metals and its color is similar to tooth color.

5.2.1 Background

The fundamental properties of zirconia ceramics which are of interest to the engineer or designer are:

- High strength,
- High fracture toughness,
- High hardness,
- Wear resistance,
- Good frictional behaviour,
- Non-magnetic,
- Electrical insulation,
- Low thermal conductivity,
- Corrosion resistance in acids and alkalis,
- Modulus of elasticity similar to steel,
- Coefficient of thermal expansion similar to iron.

5.2.2 *Types of Zirconias*

There are many different types of zirconias. These have evolved as researchers and manufacturers sought to exploit the different properties of the various phases. Some of the phases are stable at high temperatures and need to be “frozen” in such that they can be used at room temperatures, while others exploit toughening mechanisms that are only found in these and few other materials. Some of these materials are listed below along with their typical abbreviations.

Tetragonal Zirconia Polycrystals	TZP
Partially Stabilised Zirconia	PSZ
Fully Stabilised Zirconia	FSZ
Transformation Toughened Ceramics	TTC
Zirconia Toughened Alumina	ZTA
Transformation Toughened Zirconia	TTZ

Materials (oxides) added to stabilise or toughen the zirconia will also be noted as a prefix to the abbreviations listed in table 1. They will sometimes be used in conjunction with numbers which indicate the amount of the stabilising agent added. Typical examples include Y, Ce, Mg and A which correspond to yttria (Y_2O_3), ceria (CeO_2), magnesia (MgO) and alumina (Al_2O_3) respectively. So a material denoted as 3Y-TZP would tetragonal zirconia polycrystal with an addition of 3mol% Y_2O_3 as a stabiliser.

5.2.3 Property Comparison

Table 2. lists properties for various grades of zirconia and has been compiled from a variety of sources. However, as with most ceramic materials properties are dependent on many factors such as starting powders and fabrication techniques. Most ceramic fabrication techniques have been applied to zirconias such as dry pressing, isostatic pressing, injection moulding, extrusion and tape casting. Addition of impurities during processing may also introduce flaws and degrade properties.

Typical properties of various types of zirconia.

Property	Y-TZP	Ce-TZP	ZTA	Mg-PSZ	3Y20A
Density ($g.cm^{-3}$)	6.05	6.15	4.15	5.75	5.51
Hardeness (HV_{30})	1350	900	1600	1020	1470
Bend Str. (MPa)	1000	350	500	800	2400
Compressive Str. (MPa)	2000	-	-	2000	-
Young's Modulus (GPa)	205	215	380	205	260
Poisson's Ratio	0.3	-	-	0.23	-

Fracture Toughness (MPa.m ^{-1/2})	9.5	15-20	4-5	8-15	6
Thermal Exp. Co-Eff (x10 ⁻⁶ °C ⁻¹)	10	8	8	10	9.4
Thermal Conductivity (W.m ⁻¹ .K ⁻¹)	2	2	23	1.8	3

5.2.4 Yttria (Y₂O₃)

Melting point of yttria is 2410 °C. It is very stable in the air and cannot be reduced easily. It can be dissolved in acids and absorbs CO₂. It is used in Nerst lamps as filament by alloyed with zirconia and thoria in small quantities. When added to zirconia, it stabilizes the material in cubic structure. Primary yttria minerals are gadolinite, xenotime and fergusonite.

Its structure is cubic very refractory.

CHAPTER - 6

SOFTWARE'S: AN OVERVIEW

CATIA:

CATIA is one of the world's leading CAD/CAM/CAE package. Being a solid modeling tool, it not only unites 3D parametric features with 2D tools, but also addresses every design through manufacturing process.

CATIA- Computer Aided Dimensional Interactive Application.

CATIA, developed by Desalt systems, France, is a completely re-engineered, next generation family of CAD/CAM/CAE software solution.

CATIA serves the basic design task by providing different workbenches, some of the workbenches available in this package are

- Part design workbench
- Assembly design workbench
- Drafting workbench
- Wireframe and surface design workbench
- Generative shape design workbench
- DMU kinematics
- Manufacturing
- Mold design

PART DESIGN WORKBENCH

The part workbench is a parametric and feature-based environment, in which we can create solid models. In the part design workbench, we are provided with tool those convert sketches into other features are called the sketch-based features.

ASSEMBLY DESIGN WORKBENCH

The assembly design workbench is used to assemble the part by using assembly constraints. There are two type of assembly design,

- Bottom-up

➤ Top- down

In bottom –up assembly, the parts are created in part workbench and assembled in assembly workbench.

In the top-down workbench assembly, the parts are created in assembly workbench itself.

WIREFRAME AND SURFACE DESIGN WORKBENCH

The wire frame and surface design workbench is also parametric and feature based environment. The tools available in this workbench are similar to those in the part workbench, with the only difference that the tool in this environment are used to create basic and advance surfaces

DRAFTING WORKBENCH

The drafting workbench is used for the documentation of the parts or the assemblies created in the form of drafting.

There are two types of drafting techniques:

- Generative drafting
- Interactive drafting

The generative drafting technique is used to automatically generate the drawing views of parts and assemblies.

In interactive drafting, we need to create the drawing by interactive with the sketcher to generate the views.

DMU KINEMATICS

This workbench deals with the relative motion of the parts. DMU kinematics simulator is an independent CAD product dedicated to simulating assembly motions. It addresses the design review environment of digital mock-ups (DMU) and can handle a wide range of products from customer goods to very large automotive or aerospace projects as well as plants, ships and heavy machinery.

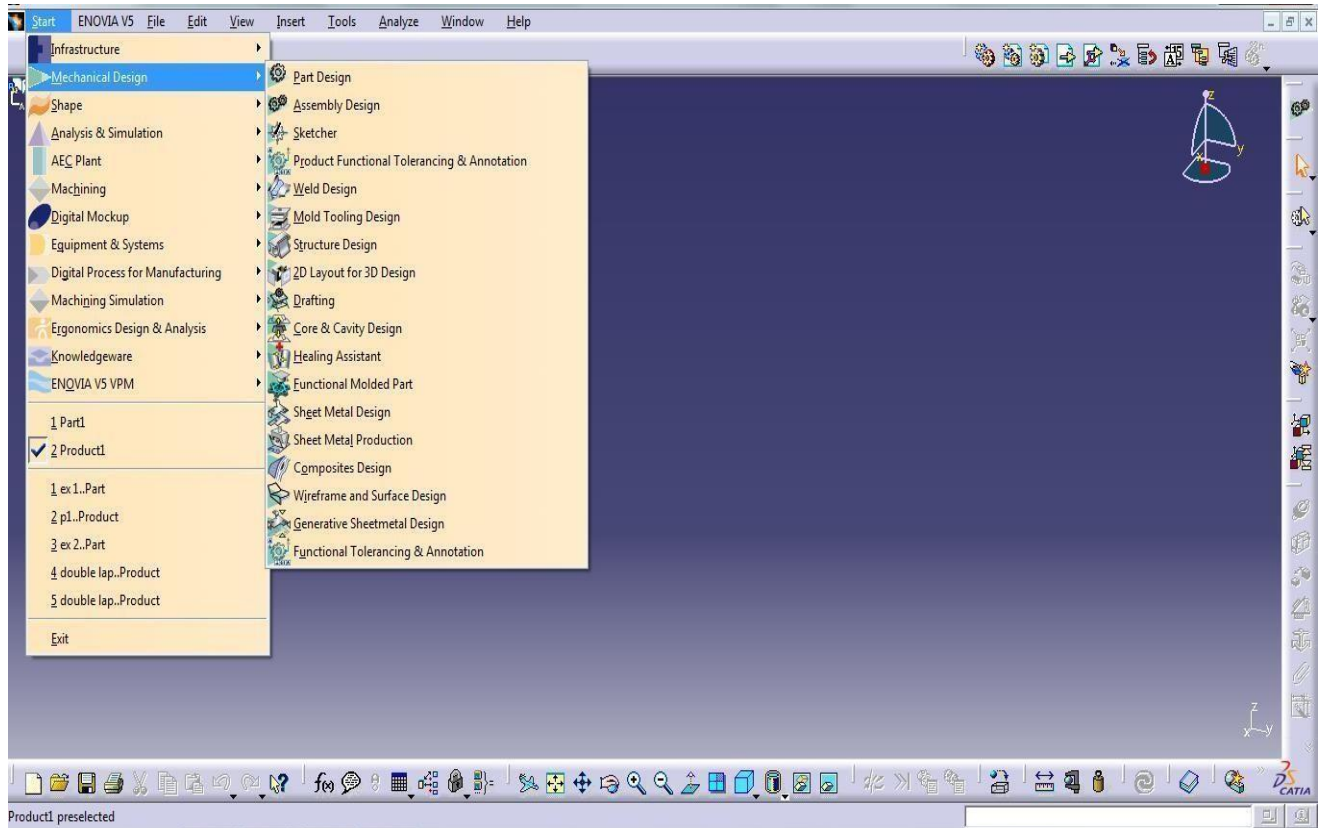


Fig. 6.1 CATIA

We created model of joints (bonded, riveted and hybrid) by using CATIA software. The models are shown below...

6.2 ANSYS EVALUATION

ANSYS is a complete FEA simulation software package developed by ANSYS Inc –USA. It is used by engineers worldwide in virtually all fields of engineering.

- StructuralA
- Thermal
- Fluid (CFD, Acoustics, and other fluid analyses)
- Low-and High-Frequency Electromagnetic.

PROCEDURE:

Every analysis involves three main steps:

- Pre-processor
- Solver
- post processor

STRUCTURAL ANALYSIS

Structural analysis is probably the most common application of the finite element method. The term structural (or structure) implies not only civil engineering structures such as bridges and buildings, but also naval, aeronautical, and mechanical structures such as ship hulls, aircraft bodies, and machine housings, as well as mechanical components such as pistons, machine parts, and tools.

TYPES OF STRUCTURAL ANALYSIS

The seven types of structural analyses available in the ANSYS family of products are explained below. The primary unknowns (nodal degrees of freedom) calculated in a structural analysis are displacements. Other quantities, such as strains, stresses, and reaction forces, are then derived from the nodal displacements.

Structural analyses are available in the ANSYS Multiphysics, ANSYS Mechanical, ANSYS Structural, and ANSYS Professional programs only.

STATIC ANALYSIS--Used to determine displacements, stresses, etc. under static loading conditions. Both linear and nonlinear static analyses. Nonlinearities can include plasticity, stress stiffening, large deflection, large strain, hyper elasticity, contact surfaces, and creep.

MODAL ANALYSIS--Used to calculate the natural frequencies and mode shapes of a structure. Different mode extraction methods are available.

HARMONIC ANALYSIS--Used to determine the response of a structure to harmonically time-varying loads.

TRANSIENT DYNAMIC ANALYSIS--Used to determine the response of a structure to arbitrarily time-varying loads. All nonlinearities mentioned under Static Analysis above are allowed.

SPECTRUM ANALYSIS--An extension of the modal analysis, used to calculate stresses and strains due to a response spectrum or a PSD input (random vibrations).

BUCKLING ANALYSIS--Used to calculate the buckling loads and determine the buckling mode shape. Both linear (eigenvalue) buckling and nonlinear buckling analyses are possible.

EXPLICIT DYNAMIC ANALYSIS--This type of structural analysis is only available in the ANSYS LS-DYNA program. ANSYS LS-DYNA provides an interface to the LS-DYNA explicit finite element program. Explicit dynamic analysis is used to calculate fast solutions for large deformation dynamics and complex contact problems.

In addition to the above analysis types, several special-purpose features are available:

- Fracture mechanics
- Composites
- Fatigue
- p-Method
- Beam Analyses

ELEMENTS USED IN STRUCTURAL ANALYSES

Most ANSYS element types are structural elements, ranging from simple spars and beams to more complex layered shells and large strain solids. Most types of structural analyses can use any of these elements.

Table	Elements	used	in	Structural	Analysis
-------	----------	------	----	------------	----------

Category	Element Name(s)
Spars	LINK1, LINK8, LINK10, LINK180
Beams	BEAM3, BEAM4, BEAM23, BEAM24, BEAM44, BEAM54, BEAM188, BEAM189
Pipes	PIPE16, PIPE17, PIPE18, PIPE20, PIPE59, PIPE60
2-D Solids	PLANE2, PLANE25, PLANE42, HYPER56, HYPER74, PLANE82, PLANE83, HYPER84, VISCO88, VISCO106, VISCO108, PLANE145, PLANE146, PLANE182, PLANE183
3-D Solids	SOLID45, SOLID46, HYPER58, SOLID64, SOLID65, HYPER86, VISCO89, SOLID92, SOLID95, VISCO107, SOLID147, SOLID148, HYPER158, SOLID185, SOLID186, SOLID187, SOLID191
Shells	SHELL28, SHELL41, SHELL43, SHELL51, SHELL61, SHELL63, SHELL91, SHELL93, SHELL99, SHELL150, SHELL181
Interface	INTER192, INTER193, INTER194, INTER195
Contact	CONTAC12, CONTAC52, TARGE169, TARGE170, CONTA171, CONTA172, CONTA173, CONTA174, CONTA175
Coupled-Field	SOLID5, PLANE13, FLUID29, FLUID30, FLUID38, SOLID62, FLUID79, FLUID80, FLUID81, SOLID98, FLUID129, INFIN110, INFIN111, FLUID116, FLUID130
Specialty	COMBIN7, LINK11, COMBIN14, MASS21, MATRIX27, COMBIN37, COMBIN39, COMBIN40, MATRIX50, SURF153, SURF154
Explicit Dynamics	LINK160, BEAM161, PLANE162, SHELL163, SOLID164, COMBI165, MASS166, LINK167, SOLID168

MATERIAL MODEL INTERFACE

If we are using the GUI, we must specify the material we will be simulating using an intuitive material model interface. This interface uses a hierarchical tree structure of material categories, which is intended to assist in us choosing the appropriate model for our analysis.

TYPES OF SOLUTION METHODS

Two solution methods are available for solving structural problems in the ANSYS family of products: the h-method and the p-method. The h-method can be used for any type of analysis, but the p-method can be used only for linear structural static analyses. Depending on the problem to be solved, the h-method usually requires a finer mesh than the p-method. The p-method provides an excellent way to solve a problem to a desired level of accuracy while using a coarse mesh. In general, the discussions in this manual focus on the procedures required for the h-method of solution.

STRUCTURAL STATIC ANALYSIS

A static analysis calculates the effects of steady loading conditions on a structure, while ignoring inertia and damping effects, such as those caused by time-varying loads. A static

analysis can, however, include steady inertia loads (such as gravity and rotational velocity), and time-varying loads that can be approximated as static equivalent loads (such as the static equivalent wind and seismic loads commonly defined in many building codes).

Static analysis is used to determine the displacements, stresses, strains, and forces in structures or components caused by loads that do not induce significant inertia and damping effects. Steady loading and response conditions are assumed; that is, the loads and the structure's response are assumed to vary slowly with respect to time. The kinds of loading that can be applied in a static analysis include:

- Externally applied forces and pressures
- Steady-state inertial forces (such as gravity or rotational velocity)
- Imposed (nonzero) displacements
- Temperatures (for thermal strain)
- Fluences (for nuclear swelling)

PERFORMING A STATIC ANALYSIS

The procedure for a static analysis consists of these tasks:

- Build the Model
- Set Solution Controls
- Set Additional Solution Options
- Apply the Loads
- Solve the Analysis
- Review the Results

LOAD TYPES

All of the following load types are applicable in a static analysis.

DISPLACEMENTS (UX, UY, UZ, ROTX, ROTY, ROTZ)

These are DOF constraints usually specified at model boundaries to define rigid support points. They can also indicate symmetry boundary conditions and points of known motion. The directions implied by the labels are in the nodal coordinate system.

FORCES (FX, FY, FZ) AND MOMENTS (MX, MY, MZ)

These are concentrated loads usually specified on the model exterior. The directions implied by the labels are in the nodal coordinate system.

PRESSURES (PRES)

These are surface loads, also usually applied on the model exterior. Positive values of pressure act towards the element face (resulting in a compressive effect).

TEMPERATURES (TEMP)

These are applied to study the effects of thermal expansion or contraction (that is, thermal stresses). The coefficient of thermal expansion must be defined if thermal strains are to be calculated. We can read in temperatures from a thermal analysis [LDREAD], or we can specify temperatures directly, using the BF family of commands.

FLUENCES (FLUE)

These are applied to study the effects of swelling (material enlargement due to neutron bombardment or other causes) or creep.

GRAVITY, SPINNING, ETC.

These are inertia loads that affect the entire structure. Density (or mass in some form) must be defined if inertia effects are to be included.

APPLY LOADS TO THE MODEL

Except for inertia loads, which are independent of the model, we can define loads either on the solid model (key points, lines, and areas) or on the finite element model (nodes and elements). We can also apply boundary conditions via TABLE type array parameters. Applying Loads Using TABLE Type Array Parameters) or as function boundary conditions

5.3 ELEMENT TYPE USED IN THE PROJECT

SOLID45 Element Description

SOLID45 is used for the 3-D modeling of solid structures. The element is defined by eight nodes having three degrees of freedom at each node: translations in the nodal x, y, and z directions.

The element has plasticity, creep, swelling, stress stiffening, large deflection, and large strain capabilities.

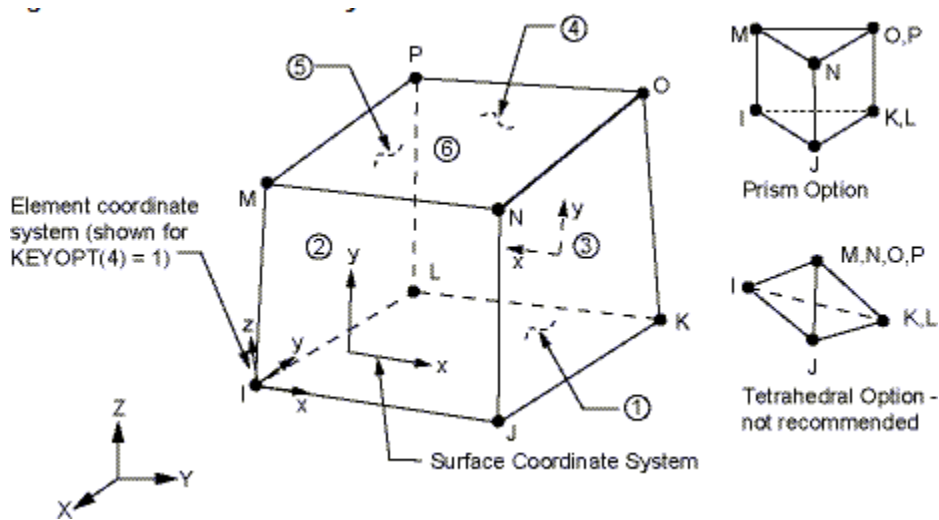


Fig. 5.2 SOLID45 Geometry

TARGE170 Element Description

TARGE170 is used to represent various 3-D "target" surfaces for the associated contact elements (CONTA173, CONTA174, CONTA175, CONTA176 & CONTA177). The contact elements themselves overlay the solid, shell, or line elements describing the boundary of a deformable body and are potentially in contact with the target surface, defined by TARGE170. This target surface is discretized by a set of target segment elements (TARGE170) and is paired with its associated contact surface via a shared real constant set. We can impose any translational or rotational displacement, temperature, voltage, and magnetic potential on the target segment element. we can also impose forces and moments on target elements.

For rigid target surfaces, these elements can easily model complex target shapes. For flexible targets, these elements will overlay the solid, shell, or line elements describing the boundary of the deformable target body.

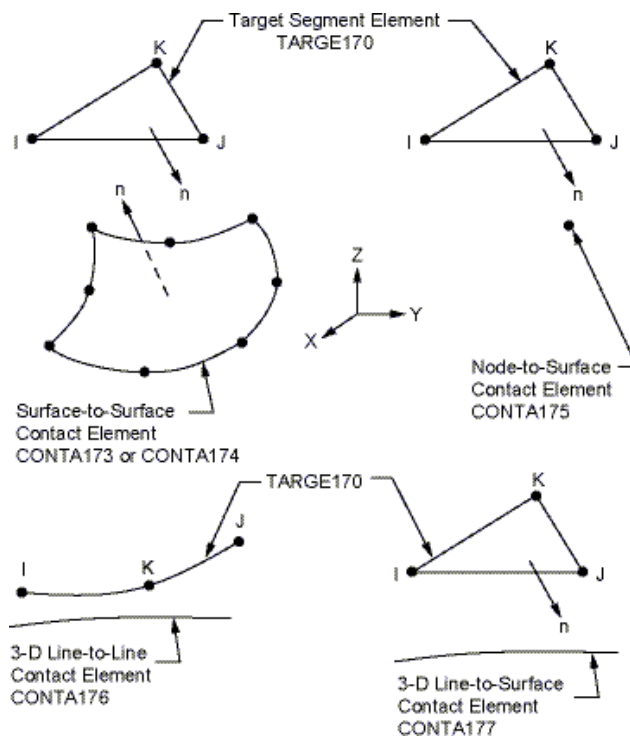


Fig. 5.3 TARGE170 Geometry

6.1 MODELS AND DRAWING

Design

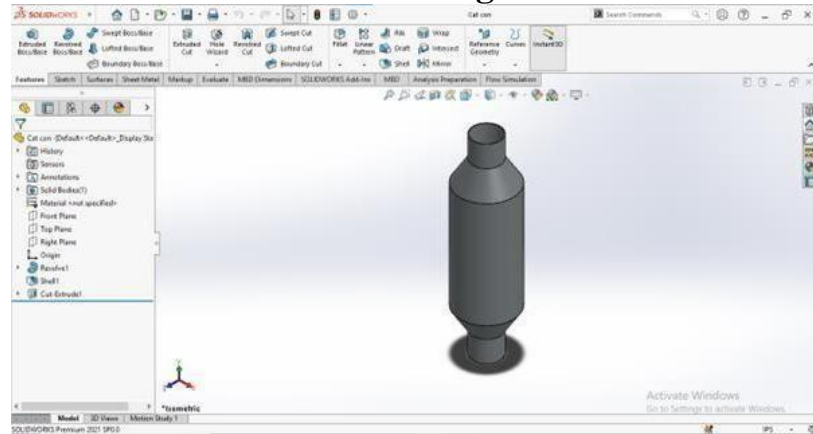


Fig. 6.1 Isometric View

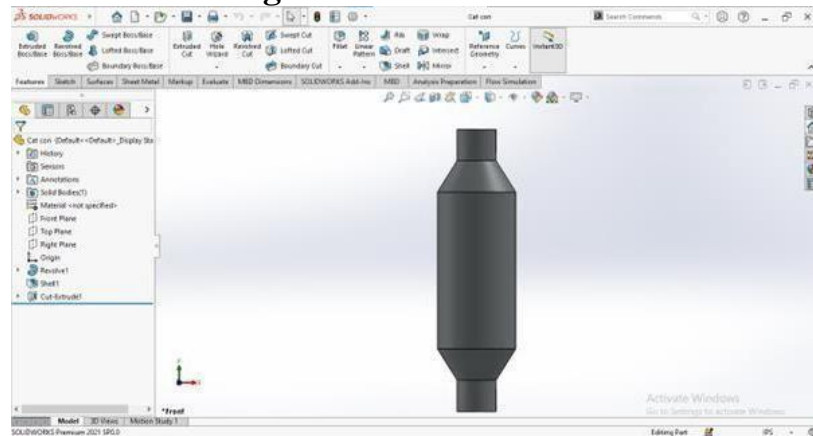


Fig. 6.2 Front View

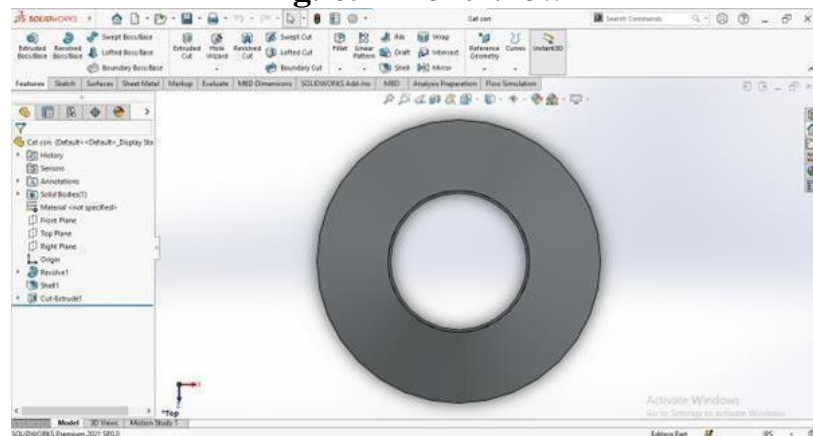


Fig. 6.3 Top View

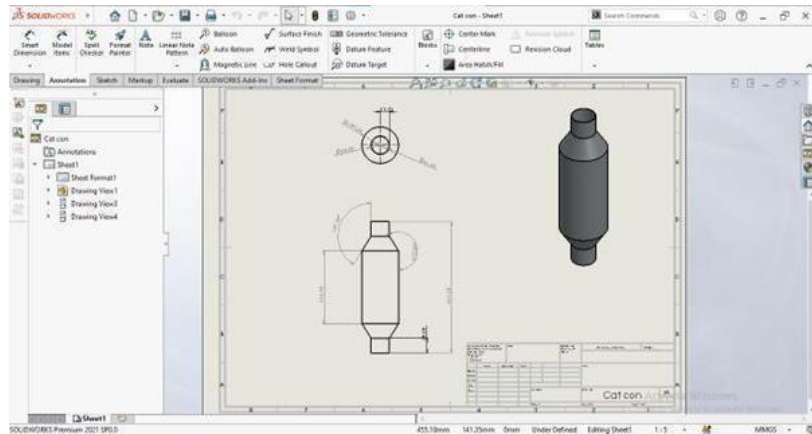


Fig. 6.4 2D Drawing

6.2 Analysis Analysis Results

Outline of Schematic A2: Engineering Data				
	A	B	C	D
1	Contents of Engineering Data			Source
2	Material			Description
3	Alumina			C:\Users\user\Desktop\Engine
4	Structural Steel			General_Materials.xml
5	Titania			C:\Users\user\Desktop\Engine
6	Zirconia			C:\Users\user\Desktop\Engine
*	Click here to add a new material			

Properties of Outline Row 4: Structural Steel				
	A	B	C	D
1	Property	Value	Unit	
2	Material Field Variables	Table		
3	Isotropic Thermal Conductivity	60.5	W m ⁻¹ C ⁻¹	

Fig. 6.5 Material Property

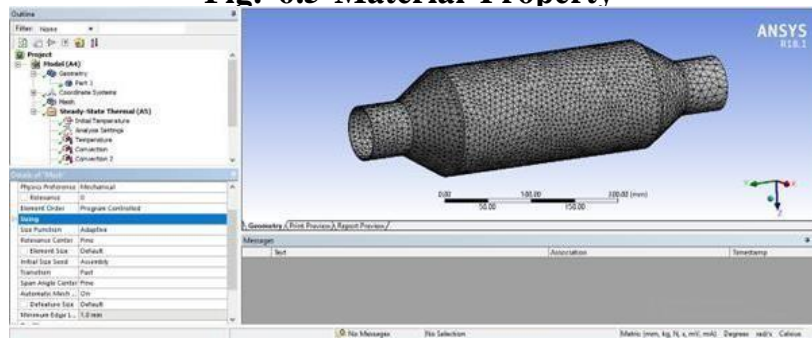


Fig. 6.6 Mesh

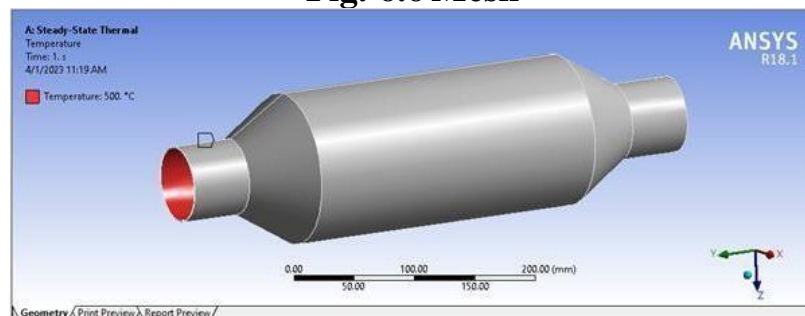


Fig.6.7 Temperature

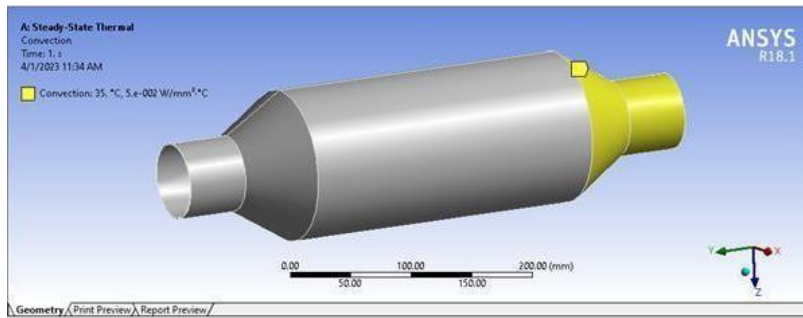


Fig.7.8 Convection 1

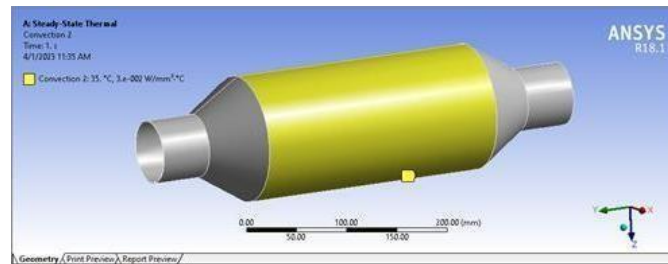


Fig.6.8 Convection 2

Results

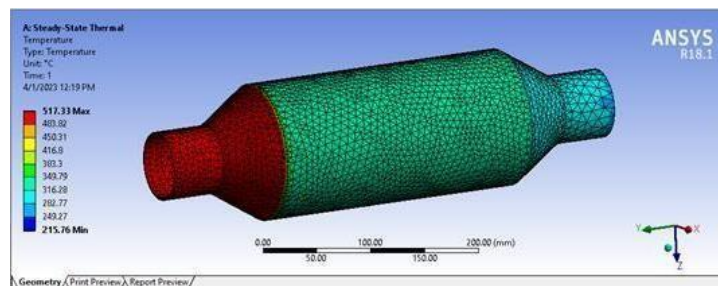


Fig.6.10 Temperature

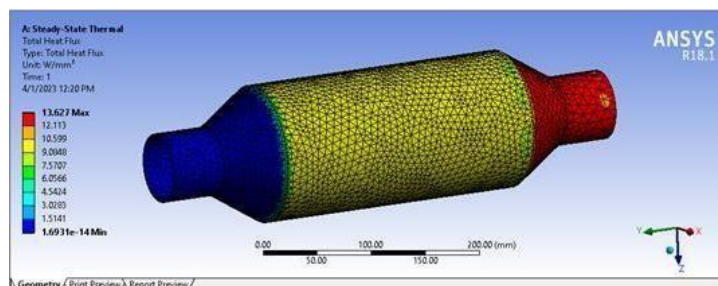


Fig.6.11 Total Heat flux

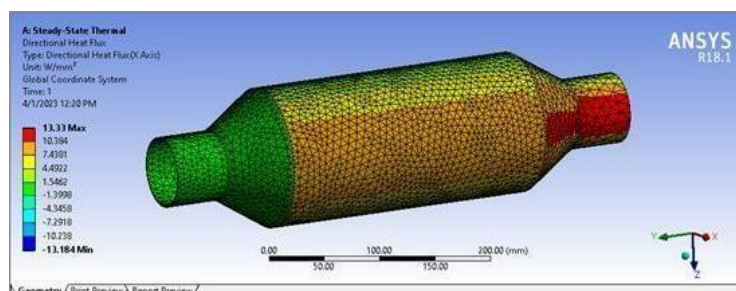


Fig.6.12 Directional heat flux

Alumina Coated Results

Outline of Schematic A2: Engineering Data				
	A	B	C	D
1	Contents of Engineering Data		Source	Description
2	Material			
3	Alumina		C:\Users\User\Desktop\Engineer	
4	Structural Steel		General_Materials.xml	from 2000 ASME BPV Code
5	Titania		C:\Users\User\Desktop\Engineer	
6	Zirconia		C:\Users\User\Desktop\Engineer	
*	Click here to add a new material			

Properties of Outline Row 3: Alumina			
	A	B	C
1	Property	Value	Unit
2	Material Field Variables	Table	
3	Isotropic Thermal Conductivity	38.5	W m ⁻¹ C ⁻¹

6.13 Material Property

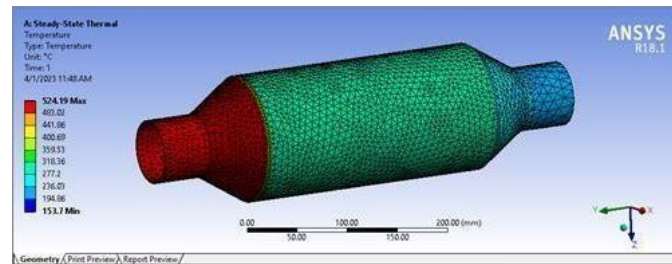


Fig.6.14 Temperature

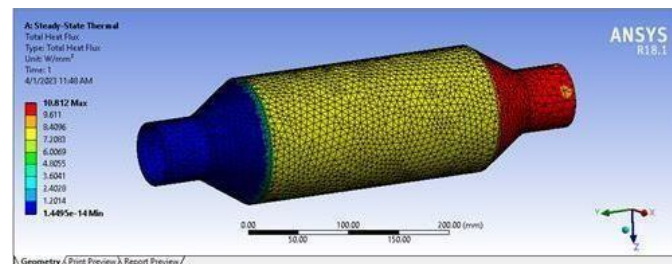


Fig.6.15 Total Heat flux

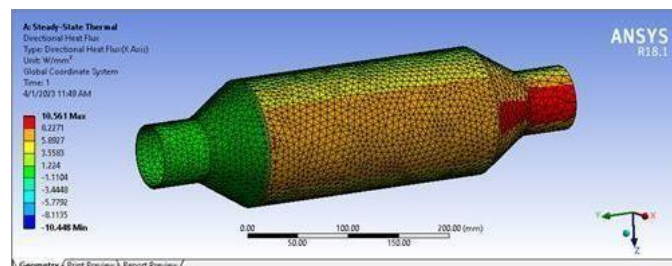


Fig.6.16 Directional Heat flux

Titania Coated Results

Outline of Schematic A2: Engineering Data				
	A	B	C	D
1	Contents of Engineering Data		Source	Description
2	Material			
3	Alumina		C:\Users\User\Desktop\Engineer	
4	Structural Steel		General_Materials.xml	from 2000 ASME BPV Code
5	Titania		C:\Users\User\Desktop\Engineer	
6	Zirconia		C:\Users\User\Desktop\Engineer	
*	Click here to add a new material			

Properties of Outline Row 5: Titania			
	A	B	C
1	Property	Value	Unit
2	Material Field Variables	Table	
3	Isotropic Thermal Conductivity	4.8	W m ⁻¹ C ⁻¹

6.17 Material Property

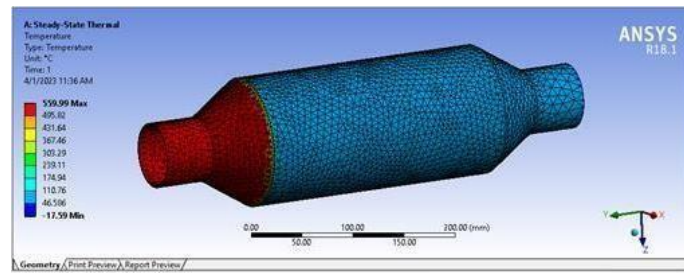


Fig.6.18 Temperature

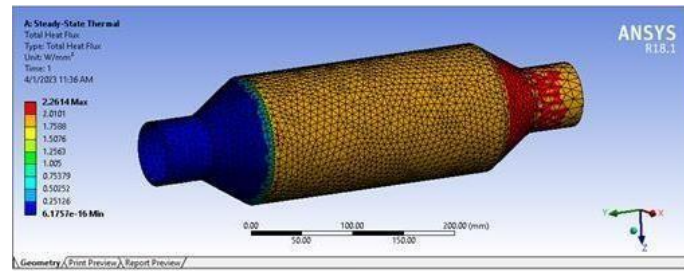


Fig.6.19 Total Heat Flux

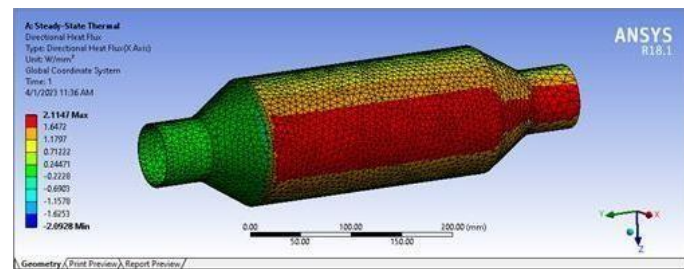


Fig.6.20 Directional Heat flux

Zirconia Coated Results

Outline of Schematic A2: Engineering Data					
	A	B	C	D	E
1	Contents of Engineering Data		Source	Description	
2	Material				
3	Alumina		C:\Users\Luser\Desktop\Engne		
4	Structural Steel		General_Materials.xml		ASME BPV Code
5	Titanium		C:\Users\Luser\Desktop\Engne		
6	Zirconia		C:\Users\Luser\Desktop\Engne		
	Click here to add a new material				
Properties of Outline Item A2: Zirconia					
	A	B	C	D	E
1	Property		Value	Unit	
2	Material Field Variables		Table		
3	Isotropic Thermal Conductivity		5	W m ⁻¹ C ⁻¹	

Fig.6.21 Material Property

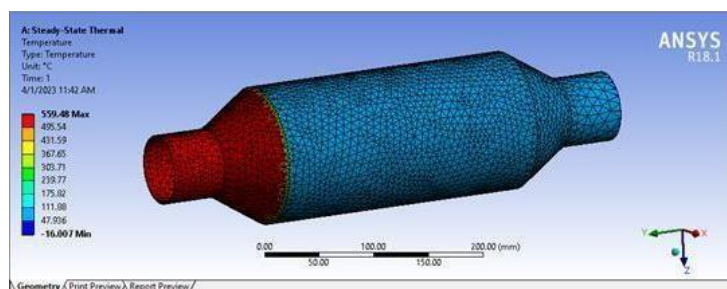


Fig.6.21 Temperature

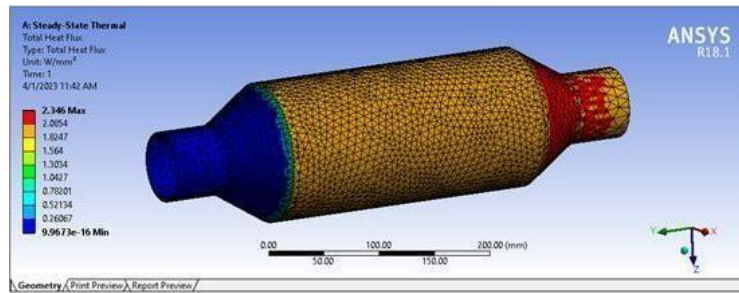


Fig.6.22 Total Heat flux

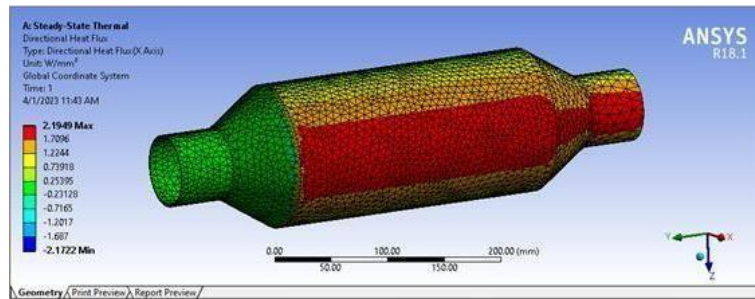
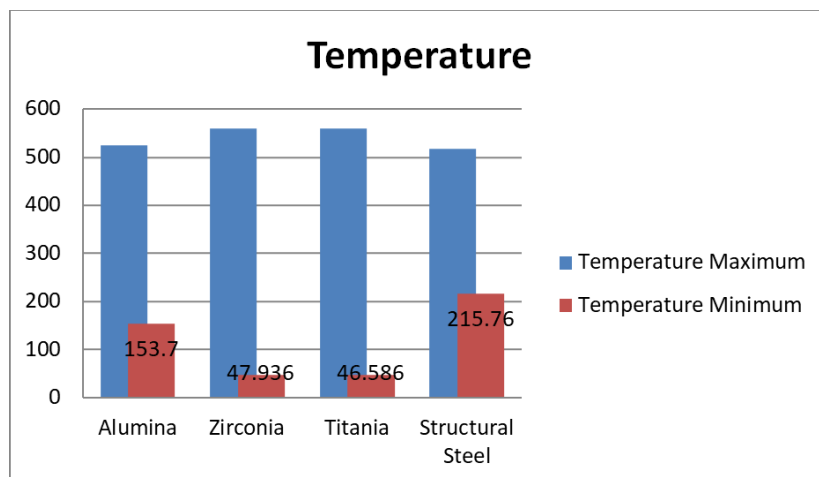


Fig.6.23 Directional Heat flux

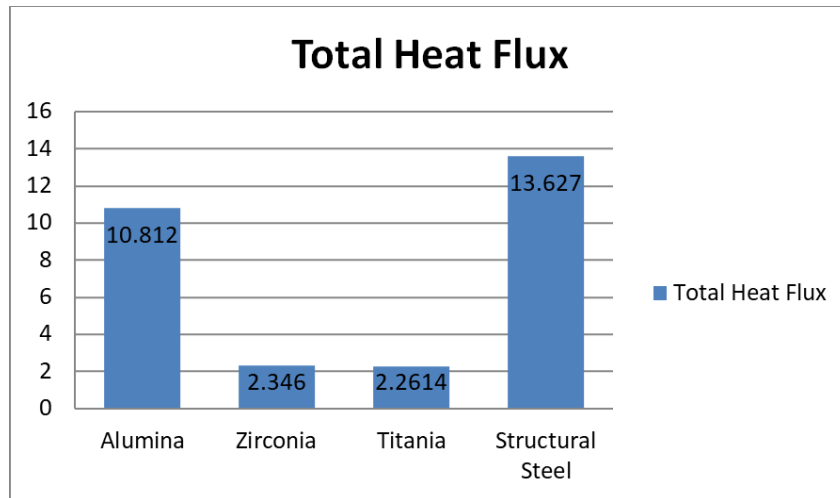
6.3 Comparison of analysis

	Temperature	
	Maximum	Minimum
Alumina	524.19	153.7
Zirconia	559.48	47.936
Titania	559.99	46.586
Structural Steel	517.33	215.76

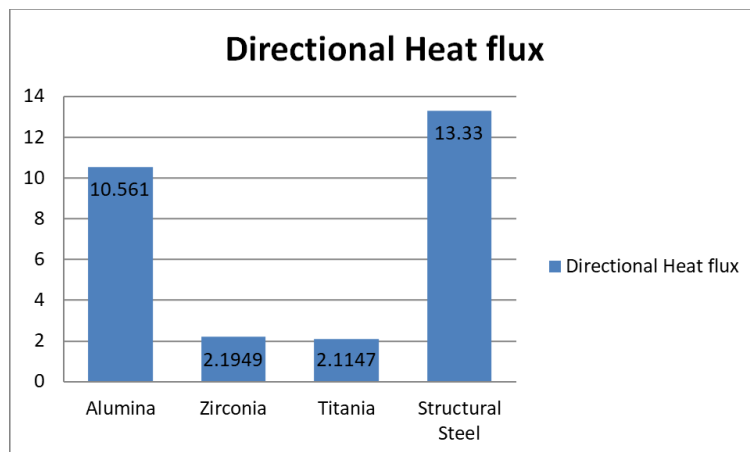


	Total Heat Flux
Alumina	10.812
Zirconia	2.346

Titania	2.2614
Structural Steel	13.627



	Directional Heat flux
Alumina	10.561
Zirconia	2.1949
Titania	2.1147
Structural Steel	13.33



Finding from Numerical Investigation:

When all of the data and graphs are examined, it is clear that the coatings made of titania provide the most effective outcomes compared to both coated and uncoated materials. When compared to the temperatures of other materials, both the material's maximum and lowest temperatures perform well. Titania's substance has seen a reduction in the overall heat flux, which indicates that the

total heat flow has been managed. Titania is a good candidate for the substance that will cover the catalytic converter, and we recommend using it. Based on the obtained best results from the numerical analysis , the coating on sample , and conduct the mechanical, corrosion and microstructural characterization.

CHAPTER - 7

EXPERIMENTAL WORK

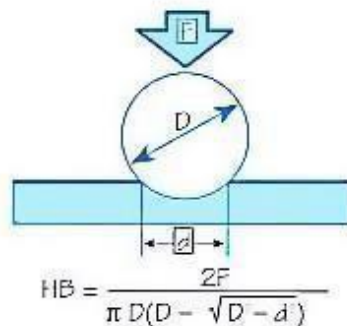
7.1 BRINELL HARDNESS

Hardness is a characteristic of a material, not a fundamental physical property. It is defined as the resistance to indentation, and it is determined by measuring the permanent depth of the indentation.

The **Brinell hardness test method** as used to determine Brinell hardness, is defined in ASTM E10. Most commonly it is used to test materials that have a structure that is too coarse or that have a surface that is too rough to be tested using another test method, e.g., castings and forgings. Brinell testing often use a very high test load (3000 kgf) and a 10mm diameter indenter so that the resulting indentation averages out most surface and sub-surface inconsistencies.

The Brinell method applies a predetermined test load (F) to a carbide ball of fixed diameter (D) which is held for a predetermined time period and then removed. The resulting impression is measured with a specially designed Brinell microscope or optical system across at least two diameters – usually at right angles to each other and these results are averaged (d). Although the calculation below can be used to generate the Brinell number, most often a chart is then used to convert the averaged diameter measurement to a Brinell hardness number.

Common test forces range from 500kgf often used for non-ferrous materials to 3000kgf usually used for steels and cast iron. There are other Brinell scales with load as low as 1kgf and 1mm diameter indenters but these are infrequently used.



Test Method Illustration

D = Ball diameter

d = impression diameter

F = load

HB = Brinell result

Typically the greatest source of error in Brinell testing is the measurement of the indentation. Due to disparities in operators making the measurements, the results will vary even under perfect conditions. Less than perfect conditions can cause the variation to increase greatly. Frequently the test surface is prepared with a grinder to remove surface conditions.

The jagged edge makes interpretation of the indentation difficult. Furthermore, when operators know the specifications limits for rejects, they may often be influenced to see the measurements in a way that increases the percentage of “good” tests and less re-testing.

Two types of technological remedies for countering Brinell measurement error problems have been developed over the years. Automatic optical Brinell scopes, such as the B.O.S.S. system, use computers and image analysis to read the indentations in a consistent manner. This standardization helps eliminate operator subjectivity so operators are less-prone to automatically view in-tolerance results when the sample’s result may be out-of-tolerance.

Brinell units, which measure according to ASTM E103, measure the samples using Brinell hardness parameters together with a Rockwell hardness method. This method provides the most repeatable results (and greater speed) since the vagaries of optical interpretations are removed through the use of an automatic mechanical depth measurement.

Using this method, however, results may not be strictly consistent with Brinell results due to the different test methods – an offset to the results may be required for some materials. It is easy to establish the correct values in those cases where this may be a problem

7.2 SALT SPRAY TEST

The salt spray test is a standardized test method used to check corrosion resistance of coated samples. Coatings provide corrosion resistance to metallic parts made of steel, zinc or brass. Since coatings can provide a high corrosion resistance through the intended life of the part in use, it is necessary to check corrosion resistance by other means. Salt spray test is an

accelerated corrosion test that produces a corrosive attack to the coated samples in order to predict its suitability in use as a protective finish. The appearance of corrosion products (oxides) is evaluated after a period of time. Test duration depends on the corrosion resistance of the coating; the more corrosion resistant the coating is, the longer the period in testing without showing signs of corrosion.

Salt spray testing is popular because it is cheap, quick, well standardized and reasonably repeatable. There is, however, only a weak correlation between the duration in salt spray test and the expected life of a coating (especially on hot dip galvanized steel where drying cycles are important for durability), since corrosion is a very complicated process and can be influenced by many external factors. Nevertheless, salt spray test is widely used in the industrial sector for the evaluation of corrosion resistance of finished surfaces or parts.

The **salt spray test** is a standardized and popular corrosion **test** method, used to check corrosion resistance of materials and surface coatings. Usually, the materials to be tested are metallic and finished with a surface coating which is intended to provide a degree of corrosion protection to the underlying metal.

Salt spray testing is an accelerated corrosion test that produces a corrosive attack to coated samples in order to evaluate (mostly comparatively) the suitability of the coating for use as a protective finish. The appearance of corrosion products (rust) is evaluated after a pre-determined period of time. Test duration depends on the corrosion resistance of the coating; generally, the more corrosion resistant the coating is, the longer the period of testing before the appearance of corrosion/ rust. The salt spray test is one of the most widespread and long established corrosion tests. ASTM B117 was the first internationally recognized salt spray standard, originally published in 1939. Other important relevant standards are ISO9227, JIS Z 2371 and ASTM G85

7.2.1 Testing equipment



Fig.7.1 Salt spry chamber for Corrosion test

7.2.2 Salt spray cabinet

The apparatus for testing consists of a closed testing chamber, where a salted solution (mainly, a solution of 5% sodium chloride) is atomized by means of a nozzle. This produces a corrosive environment of dense saline fog in the chamber so that parts exposed in it are subjected to severely corrosive conditions. Typical volumes of these chambers are of 15 cubic feet (420 L) because of the smallest volume accepted by International Standards on Salt Spray Tests - ASTM-B-117, ISO 9227 and now discontinued DIN 50021 (400 litres). It has been found very difficult to attain constancy of corrosivity in different exposure regions within the test chambers, for sizes below 400 litres. Chambers are available from sizes as small as 4.3 cu ft (120 L) up to 2,058 cubic feet (58,300 L). Most common machines range from 15 to 160 cubic feet (420–4,530 L).

Tests performed with a standardized 5% solution of NaCl are known as NSS (neutral salt spray). Results are represented generally as testing hours in NSS without appearance of corrosion products (e.g. 720 h in NSS according to ISO 9227). Other solutions are acetic acid (ASS test) and acetic acid with copper chloride (CASS test), each one chosen for the evaluation of decorative coatings, such as electroplated copper-nickel-chromium, electroplated copper-nickel or anodized aluminium.

Some sources do not recommend to use ASS or CASS test cabinets interchangeably for NSS tests, as it is claimed that a thorough cleaning of the cabinet after ASS or CASS test is very difficult. ASTM does not address this issue, but ISO 9227 does not recommend it and if it is to be done, advocates a thorough cleaning.

Chamber construction, testing procedure and testing parameters are standardized under national and international standards, such as ASTM B 117 and ISO 9227. These standards describe the necessary information to carry out this test; testing parameters such as temperature, air pressure of the sprayed solution, preparation of the spraying solution, concentration, pH, etc. Daily checking of testing parameters is necessary to show compliance with the standards, so records shall be maintained accordingly. ASTM B 117 and ISO 9227 are widely used as reference standards. Testing cabinets are manufactured according to the specified requirements here. However, these testing standards neither provide information of testing periods for the coatings to be evaluated, nor the appearance of corrosion products in form of salts. Requirements shall be agreed between customer and manufacturer. In the automotive industry requirements are specified under material specifications. Different coatings have different behaviour in salt spray test and consequently, test duration will differ from one type of coating to another. For example, a typical electroplated zinc and yellow passivated steel part lasts 96 hours in salt spray test without white rust. Electroplated zinc-nickel steel parts can last more than 720 hours in NSS test without red rust (or 48 hours in CASS test without red rust) Requirements are established in test duration (hours) and coatings shall comply with minimum testing periods.

Artificial seawater which is used for Salt Spray Testing can be found at ASTM International. The standard for Artificial Seawater is ASTM D1141-98 which is the standard practice for the preparation of substitute ocean water.

Uses Typical coatings that can be evaluated with this method are:

- Phosphated surfaces (with subsequent paint/primer/lacquer/rust preventive)
- Zinc and zinc-alloy plating (see also electroplating). See ISO 4042 for guidance
- Electroplated chromium, nickel, copper, tin
- Coatings not applied electrolytically, such as zinc flake coatings according to ISO 10683
- Organic coatings

Hot-dip galvanized surfaces are not generally tested in a salt spray test (see ISO 1461 or ISO 10684). Hot-dip galvanizing produces zinc carbonates when exposed to a natural environment, thus protecting the coating metal and reducing the corrosion rate. The zinc carbonates are not produced when a hot-dip galvanized specimen is exposed to a salt spray fog, therefore this testing method does not give an accurate measurement of corrosion protection. ISO 9223 gives the guidelines for proper measurement of corrosion resistance for hot-dip galvanized specimens.

Painted surfaces with an underlying hot-dip galvanized coating can be tested according to this method. See ISO 12944-6.

Testing periods range from a few hours (e.g. 8 or 24 hours of phosphated steel) to more than a month (e.g. 720 hours of zinc-nickel coatings, 1000 hours of certain zinc flake coatings).

7.3 MICROSTRUCTURE

Microstructure is defined as the structure of a prepared surface or thin foil of material as revealed by a microscope above 25× magnification. The microstructure of a material (which can be broadly classified into metallic, polymeric, ceramic and composite) can strongly influence physical properties such as strength, toughness, ductility, hardness, corrosion resistance, high/low temperature behavior, wear resistance, and so on, which in turn govern the application of these materials in industrial practice.

Methods

The concept of microstructure is perhaps more accessible to the casual observer through macrostructural features in commonplace objects. If one ever comes across a piece of galvanized steel, such as the casing of a lamp post or road divider, one observes that the surface is not uniformly colored, but is covered with a patchwork of interlocking polygons of different shades of grey or silver. Each polygon (the most frequently occurring would be hexagons) is a single crystal of zinc adhering to the surface of the steel beneath. Zinc and lead are two common metals which form large crystals visible to the naked eye. The metallic atoms in each crystal are well-organized into one of seven crystal lattice systems possible for metals (cubic, tetrahedral, hexagonal, monoclinic, triclinic, rhombohedral, orthorhombic); these systems dictate that the atoms are all lined up like points in a 3-D matrix. However, the direction of

alignment of the matrices differ from crystal to adjacent crystal, leading to variance in the reflectivity of each presented face of the interlocked crystals on the galvanized surface. Symmetrical crystals are generally unstressed, unworked. They grow in all directions equally and were not subjected to deforming stresses either during or after. For large crystals, the ratio of crystal bulk to inter-crystal boundary (more properly, intergranular boundary) is high. This indicates high ductility but correspondingly, lower strength (see Hall-Petch Strengthening), but a true study would take into quantitative account the relative strengths of the crystal and that of inter-crystal bonding.

7.3.1 Microscopy

Optical

When a polished flat sample reveals traces of its microstructure, it is normal to capture the image using macrophotography. More sophisticated microstructure examination involves higher powered instruments: optical microscopy, electron microscopy, X-ray diffraction and so on, some involving preparation of the material sample (cutting, microtomy, polishing, etching, vapor-deposition etc.). The methods are known collectively as metallography as applied to metals and alloys, and can be used in modified form for any other material, such as ceramics, glasses, composites, and polymers.

Two kinds of optical microscope are generally used to examine flat, polished and etched specimens: a reflection microscope and an inverted microscope. Recording the image is achieved using a digital camera working through the eyepiece.

7.3.2 X-Ray microtomographic

Nondestructive testing of microstructure for biological materials is a challenge and computer microtomography is the current solution. In fact, CMT can be used for the evaluation of microstructure of many other materials also. CMT can be very expensive though, and for research purposes, it is a necessity to generate a three-dimensional microstructure from two-dimensional cross-sectional images of the material. This is an area of active research and pursued by many scientists.

7.3.2 Electron Microscopy



Aluminium copper (4 at% Cu) alloy showing copper precipitation within the aluminium matrix. The image is a projection through the metal where the dark regions are plate like copper precipitates

For high-resolution information on metallurgical microstructures, electron microscopic methods can be employed. This can allow for direct observation of atomic-scale features such as very fine precipitation reactions, dislocations or grain-boundary interfaces. Such methods may be critical in determining parameters such as solid state diffusivities

7.3.3 OPTICAL MICROSCOPY

The optical microscope, often referred to as the "light microscope", is a type of microscope which uses visible light and a system of lenses to magnify images of small samples. Optical microscopes are the oldest design of microscope and were possibly invented in their present compound form in the 17th century. Basic optical microscopes can be very simple, although there are many complex designs which aim to improve resolution and sample contrast.

The image from an optical microscope can be captured by normal light-sensitive cameras to generate a micrograph. Originally images were captured by photographic film but modern developments in CMOS and charge-coupled device (CCD) cameras allow the capture of digital images. Purely digital microscopes are now available which use a CCD camera to examine a sample, showing the resulting image directly on a computer screen without the need for eyepieces.

Alternatives to optical microscopy which do not use visible light include scanning electron microscopy and transmission electron microscopy.



Fig. 7.2 Optical configurations

7.4 TEST RESULTS

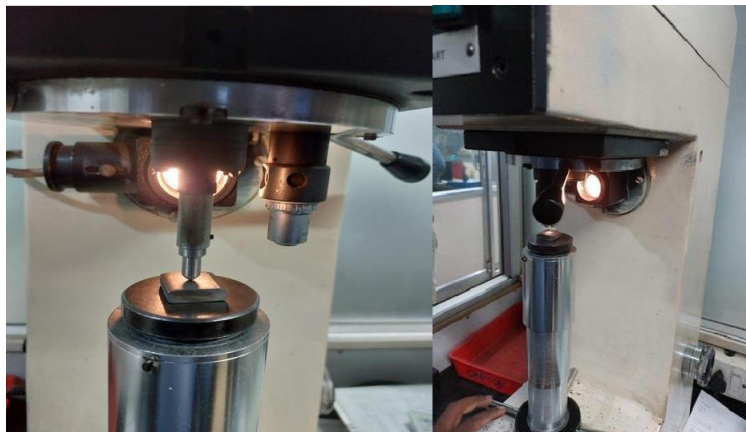


Fig.

Fig.



Fig.



Fig.



Fig.



Fig.

7.4.1 Vickers Hardness Test: (ASTM E92-2017)

Table: Vickers hardness test

Test parameters (HV 10kg)	Observed values
Coated	213, 210, 207
Uncoated	173,175,177

Vickers Hardness (ASTM E92-2017)	
SS Sample uncoated	SS Sample Coated with Titania
175	210

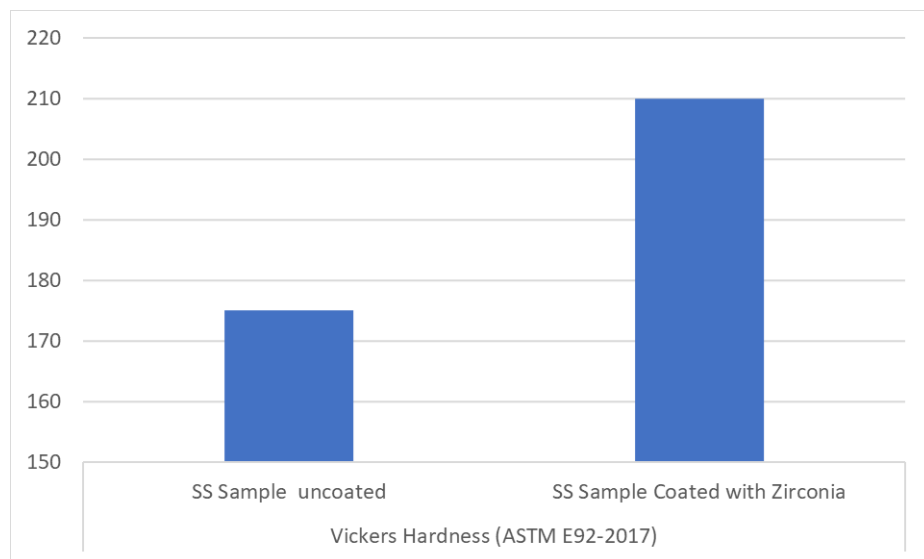


Fig.7.3 Vickers hardness

7.4.2 Microstructure Results

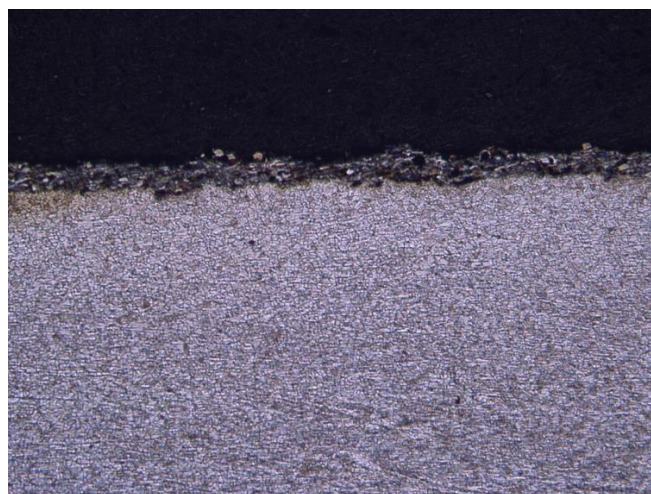


Fig: Coated Sampe Microstruture results



Fig: Bond Coated image

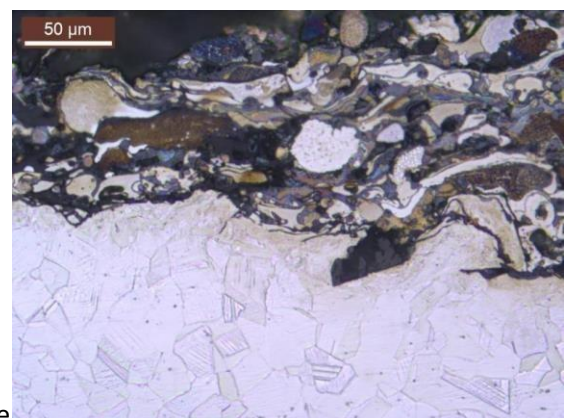


Fig: Coated with bond and ceramic coated and un-coated sample

7.4.3 Corrosion Test : un-coated sample

Neutral Salt spray	ASTM-B-117-2019	
Test parameter	Specified value	Observation
Test Duration (Hours)	24Hrs	24Hrs
Test starting date (DD/MM/YY)		23/03/23
Test ending date (DD/MM/YY)		24/03/23
Tower Temperature (*C)		47.5-48.5
Air Pressure (Psi)		14-18
Chamber Temperature(*C)		Chamber temperature(*C)
Components Loading in Chamber		15-30 Degree from vertical
Position (Degree Angle)		
Concentration of Solution (%)		4.80-5.30% of Nacl
pH value		6.65-6.85
Volume of salt solution collected (ml/hr)		1.00-1.50
Test Observation		

SS Sample Coated with Zirconia

Netural Salt Spray	ASTM-B-117-2019	
Test parameter	Specified value	<u>Observation</u>
Test Duration (Hours)	24Hrs	24Hrs
Test starting date (DD/MM/YY)		23/03/23
Test ending date (DD/MM/YY)		24/03/23
Tower temperature (*C)		47.5-48.5
Air pressure (Psi)		14-18
Chamber Temperature (*C)		Chamber temperature (*C)
Components loading in Chamber		15-30 Degree from vertical
Position (Degree Angle)		
Concentration of Solution (%)		4.80-5.30% of Nacl
pH value		6.65-6.85
Volume of salt solution collected (ml/hr)		1.00-1.50
Test observation		No Rust formation noticed up to 24 Hrs.

CHAPTER - 8

CONCLUSION

The effectiveness of the catalytic model's conversion is dependent on the temperature of the gas being introduced and the mass flow rates. In comparison to a gas temperature that is lower at the point of entry, a higher temperature at the point of entry results in a greater conversion efficiency across the board. Ceramic coating powders of several types, including alumina, titania, and zirconia, are utilised in the process of designing and analysing the catalytic converters. The use of coated catalytic converters, as opposed to uncoated ones, produced better results in terms of their thermal characteristics, which in turn led to a reduction in emissions. A catalyst that, in order to decrease to harmful gases that pollute the environment, must go through the processes of oxidation and reduction. According to the findings, the thermal nature of the newly developed type of coated catalytic converters makes it possible to manage emissions. In addition, the ceramic coating on the catalytic converter offered a heat barrier, as well as resistance to wear and corrosion. Because of this, the longevity of the catalytic converter was improved.

REFERENCE

1. B. N. Duncan, L. N. Lamsal, A. M. Thompson, Y. Yoshida, Z. Lu, D. G. Streets, M. M. Hurwitz, and K. E. Pickering, *J. Geophys. Res. Atmos.* 121 (2015) 976-996.
2. Z. Liu, H. Su, B. Chen, J. Li, and S. I. Woo, *Chem. Eng. J.* 299 (2016) 255-262.
3. W. Xie, Y. Yu, and H. He, *J. Environ. Sci.* 75 (2019) 396- 407.
4. R. Yang, Y. Cui, Q. Yan Q, C. Zhang, L. Qiu, D. O'Hare, and Q. Wang, *Chem. Eng. J.* 326 (2017) 656-666.
5. A. B. López, D. L. Castelló, and J. A. Anderson, *Appl. Catal., B.* 198 (2016) 189-199.
6. M. Li, V. G. Easterling, and M. P. Harold, *Appl. Catal., B.* 184 (2016) 364-380.
7. A. W. L. Ting, V. Balakotaiah, and M. P. Harold. *Chem. Eng. J.* 370 (2019) 1493-1510.
8. I. A. Resitoglu and A. Keskin, *Int. J. Hydrogen Energy.* 42 (2017) 23389-23394.
9. D. K. Pappas, T. Boningari, P. Boolchand, and P. G. Smirniotis, *J. Catal.* 334 (2016) 1-13.
10. J Han, J. Meeprasert, P. Maitarad, S. Nammuangruk, L. Shi, and D. Zhang, *J. Phys. Chem. C.* 120 (2016) 1523- 1533.
11. Y. Zheng, D. Luss, and M. P. Harold, *SAE Int. J. Engines*, 7 (2014) 1280-1289.
12. J. Barman, S. Arora, R. Khan, and M. Parashar, *SAE Technical Paper 1* (2016) 1733.
13. A. B. López, D. L. Castelló, A. J. McCue, and J. A. Anderson, *Appl. Catal., B.* 198 (2016) 266-275.
14. Z. Zhang, B. Chen, X. Wang, L. Xu, C. Au, C. Shi, and M. Crocker, *Appl. Catal., B* 165 (2015) 232-244.
15. V. A. Santiago, A. D. Quiñonero, I. S. Basáñez, D. L. Castelló, and A. B. López, *Appl. Catal., B.* 220 (2018) 524-532.
16. E. Srinivasa Rao and P. Manohar, *J. Ceram. Process. Res.* 17 (2016) 448-453.
17. F. A. Lafossas, C. Manetas, A. Mohammadi, G. Koltsakis, M. Iida, and K. Yoshida, *AIChE J.* 63 (2017) 2117-2127.
18. J. K. Unni, D. Bhatia, V. Dutta, L. M. Das, S. Jilakara, and G. P. Subash, *SAE Int. J. Engines.* 10 (2017) 46-54.
19. K. Lee and K. W. Nam, *J. Ceram. Process. Res.* 19 (2018) 54-64.
20. X. Yuan, Y. Gao, and X. Wang, *Int. J. Engine Res.* 17 (2016) 169-178.
21. M. Han and B. Lee, *Int. J. Automot. Technol.* 16 (2015) 371-378.
22. J. S. Park, J. G. Yeo, S. C. Yang, and C. H. Cho, *J. Ceram. Process. Res.* 19 (2018) 20-24.
23. H. Gu, K. M. Chun, and S. Song, *Int. J. Hydrogen Energy.* 40 (2015) 9602-9610.

24. X. Cheng, D. Su, Z. Wang, C. Ma, and M. Wang, *Int. J. Hydrogen Energy*. 43 (2018) 21969-21981.
25. I. A. Resitoglu, A. Keskin, H. Özarslan, and H. Bulut, *Int. J. Environ. Sci. Technol.* 16 (2019) 6959-6966.
26. U. De-La-Torre, B. Pereda-Ayo, M. Moliner, and A. Corma, *Appl. Catal., B* 187 (2016) 419-4.
27. E. R. Rangel, *J Ceram. Process. Res.* 9 (2008) 61-63.
28. I. Cornejo, P. Nikrityuk, and R. E. Hayes, *Chem. Eng. Sci.* 175 (2018) 377-386.
29. C. P. Cho, Y. D. Pyo, J. Y. Jang, G. C. Kim, and Y. J. Shin, *Appl. Therm. Eng.* 110 (2017) 18-24.
30. P. Baskar, and A. Senthilkumar, *Eng. Sci. Technol.* 19 (2016) 438-443.
31. B. Pereda-Ayo, R. López-Fonseca, and J. R. GonzálezVelasco, *Appl. Catal., A*. 363 (2009) 73-80.
32. C. Agrafioti and, A. Tsetsekou, *J. Eur. Ceram. Soc.* 20 (2000) 815-824.
33. B. Pereda-Ayo, D. Duraiswami, J. A. González-Marcos, and J. R. González-Velasco, *Chem. Eng. J.* 169 (2011) 58- 67.
34. S. P. Venkatesan and P. N. Kadiresh, *Int. J. Ambient Energy*. 37 (2016) 64-67.
35. S. Yuvaraj, K. M. Kiran Babu, P. Kaleeshwaran, and S. Tamilselvan, *Lecture Notes in Mechanical Engineering*. Springer, Singapore, (2017) 231-238.
36. ThundilKaruppa Raj R. and Ramsai R., Numerical study of fluid flow and effect of inlet pipe angle In catalytic converter using CFD, *Research Journal of Recent Sciences* ISSN 22772502 Vol. 1(7), 39-44, July (2012).
37. PL.S. Muthaiah, Dr .M. Senthil kumar, Dr. S. Sendilvelan, CFD Analysis of Catalytic Converter to Reduce Particulate Matter and Achieve Limited Back Pressure in Diesel Engine, *Global Journal of Researches in Engineering*, Page 2 Vol.10 Issue 5 (Ver1.0) October 2010.
38. V.K. Pravin, K.S. Umesh, K. Rajagopal and P.H. Veena, Numerical Investigation of Various Models of Catalytic Converters in Diesel Engine to Reduce Particulate Matter and Achieve Limited Back Pressure, *International Journal of Fluids Engineering*. ISSN 0974-3138 Volume 4, Number 2 (2012), pp. 105-118.
39. Bassem H. Ramadan and Philip C. Lundberg, Characterization of a Catalytic Converter Internal Flow, SAE paper, 2007-01-4024 (2007)

40. P.Karuppusamy, Dr. R.Senthil, Design, analysis of flow characteristics of catalytic converter and effects of backpressure on engine performance, IJREAT, Volume 1, Issue 1, March, 2013
41. FLUENT Inc. FLUENT 6.0 User's Guide, FLUENT Documentation, 2001
42. Pontikakis, Georgios N. 2003, "Modeling, reaction schemes and kinetic parameter estimation in automotive catalytic converters and diesel particulate filters", University of Thessaly, Thessaloniki, PhD Thesis UTh/MIE No. 8.001, pp. 371-384. doi:10.1016/j.ijp.2003.08.001. ISSN: 2320 – 8791
43. Jinke Gong, Longyu Cai, Weiling Peng and Jingwu Liu, Yunqing Liu, Hao Cai and Jiaqiang E, Analysis to the Impact of Monolith Geometric Parameters on Emission Conversion performance Based on an Improved Threeway Catalytic Converter Simulation Model, SAE paper 2006-32-0089 (2006)
44. Howitt J.S. and Sekella T.C., Flow Effects in Monolithic automotive Catalytic Converters, SAE paper 740244, (1974)